International Journal of Nanomedicine

Dovepress
open access to scientific and medical research

Open Access Full Text Article

ORIGINAL RESEARCH

RETRACTED ARTICLE: Investigation of Eutectic Mixtures of Fatty Acids as a Novel Construct for Temperature-Responsive Drug Delivery

Farzana Parveen[1–3], Asadullah Madni[2], Vladimir P Torchilin[1], Mubashar Rehman[4], Talha Jamshaid[2], Nina Filipczak[1], Nadia Rai[2,5], Muhammad Muzamil Khan[2,3], Muhammad Imran Khan[6]

[1]Center for Pharmaceutical Biotechnology and Nanomedicine, Northeastern University, Boston, MA, 02115, USA; [2]Department of Pharmaceutics, Faculty of Pharmacy, The Islamia University of Bahawalpur, Bahawalpur, Punjab, 63100, Pakistan; [3]Primary and Secondary Healthcare Department, Government of Punjab, Lahore, 54000, Pakistan; [4]Department of Pharmacy, Quaid-i-Azam University, Islamabad, 45320, Pakistan; [5]Department of Biomedical and Pharmaceutical Sciences, Chapman University School of Pharmacy, Irvine, CA, 92618, USA; [6]Riphah Institute of Pharmaceutical Sciences, Riphah International University Lahore Campus, Lahore, 54000, Pakistan

Correspondence: Asadullah Madni, Department of Pharmaceutics, Faculty of Pharmacy, The Islamia University of Bahawalpur, Bahawalpur, Punjab, 63100, Pakistan, Tel +92 62 925 5243, Fax +92 62 925 5565, Email asadpharmacist@hotmail.com

Background: Most of the traditional nanocarriers of cancer therapeutic moieties present dose-related toxicities due to the uptake of chemotherapeutic agents in normal body cells. The severe life-threatening effects of systemic chemotherapy are well documented. Doxorubicin, DOX is the most effective antineoplastic agent but with the least specific action that is responsible for severe cardiotoxicity and myelosuppression that necessitates careful monitoring while administering. Stimuli-sensitive/intelligent drug delivery systems, specifically those utilizing temperature as an external stimulus to activate the release of encapsulated drugs, have become a subject of recent research. Thus, it would be ideal to have a nanocarrier comprising safe excipients and controllable drug release capacity to deliver the drug at a particular site to minimize unwanted and adverse effects of chemotherapeutics. We have developed a simple temperature-responsive nanocarrier based on eutectic mixture of fatty acids. This study aimed to develop, physicochemically characterize and investigate the biological safety of eutectic mixture of fatty acids as a novel construct for temperature-responsive drug release potential.

Methods: We have developed phase change material, PCM, based on a series of eutectic mixtures of fatty acids due to their unique and attractive physicochemical characteristics such as safety, stability, cost-effectiveness, and ease of availability. The reversible solid-liquid phase transition of PCM is responsible to hold firm or actively release the encapsulated drug. The eutectic mixtures of fatty acids (stearic acid and myristic acid) along with liquid lipid (oleic acid) were prepared to exhibit a tunable thermoresponsive platform. Doxorubicin-loaded lipid nanocarriers were successfully developed with combined hot melt encapsulation (HME) and sonication method and characterized to achieve enhanced permeability and retention (EPR) effect-based solid tumor targeting in response to exogenous temperature stimulus. The cytotoxicity against melanoma cell lines and in vivo safety studies in albino rats was also carried out.

Results: Doxorubicin-loaded lipid nanocarriers have a narrow size distribution (94.59–219.3 nm), and a PDI (0.160–0.479) as demonstrated by photon correlation microscopy and excellent colloidal stability (Z.P value: −22.7 to −32.0) was developed. Transmission electron microscopy revealed their spherical morphology and characteristics of a monodispersed system. A biphasic drug release pattern with a triggered drug release at 41°C and 43°C and a sustained drug release was observed at 37°C. The thermoresponsive cytotoxic potential was demonstrated in B16F10 cancer cell lines. Hemolysis assay and acute toxicity studies with drug-free and doxorubicin lipid nanocarrier formulations provided evidence for their non-toxic nature.

Conclusion: We have successfully developed a temperature-responsive tunable platform with excellent biocompatibility and intelligent drug release potential. The formulation components being from natural sources present superior characteristics in terms of cost, compatibility with normal body cells, and adaptability to preparation methods. The reported preparation method is adapted to avoid complex chemical processes and the use of organic solvents. The lipid nanocarriers with tunable thermoresponsive characteristics are promising biocompatible drug delivery systems for improved localized delivery of chemotherapeutic agents.

Keywords: nanostructured lipid carriers, lipid nanocarriers, thermoresponsive, eutectic mixtures, fatty acids, phase change materials, doxorubicin, acute toxicity studies, hemolysis assay

Received: 2 February 2022
Accepted: 11 May 2022
Published: 26 May 2022

Graphical Abstract

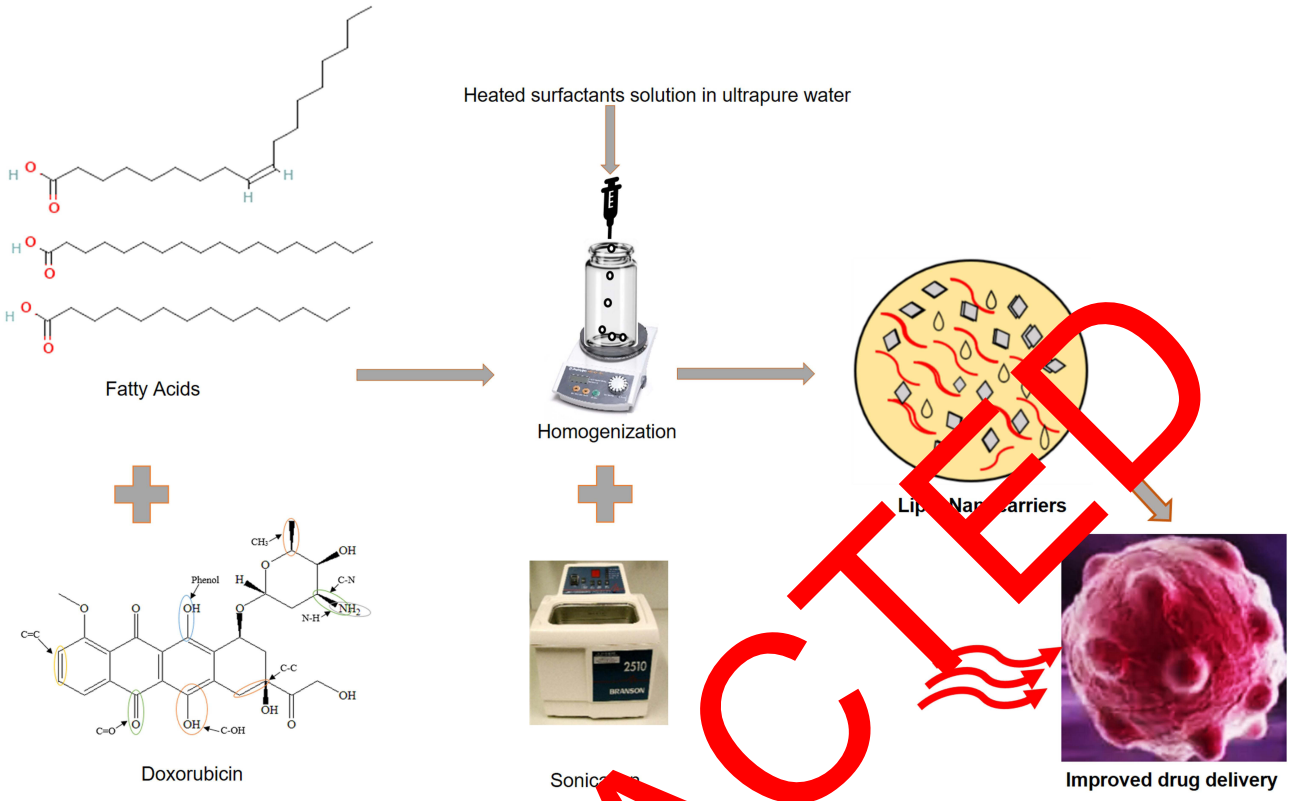

Introduction

The cancer burden 2020 estimates about 19.3 million new cases and 10 million deaths worldwide due to cancer were reported. Every sixth death was due to cancer which is the second leading cause of mortality globally. The female breast cancer incidence rate has overstepped among all types of cancer with 2.3 million new cases reported worldwide. Most of the cancer deaths were due to lung cancer (1.8 million, 18% cancer deaths) with 2.2 million new cases and 1.8 million reported deaths. Additionally, the impact of the COVID-19 pandemic in different world regions, health system closures, delays in diagnosis and treatment, suspension of screening programs, reduced availability, and access to standard care are likely to be factors that affect the early stage diagnoses and treatments.[1–3] The incidence rates of different types of cancer may also vary across the countries depending upon the degree of economic development as well as social and lifestyle factors.[4] Most of conventional chemotherapeutics lack specificity and cause life-threatening toxicities due to inhibition of normal cell division. The next generation of cancer therapy requires the drugs to behave more precisely and specifically to avoid side effects on normal cells with high rates of division located in bone marrow, hair follicles, and digestive tract.[5]

Smart drug delivery systems, DDS have gained more attention to overcome non-specific bio-distribution and release payloads in a spatially controlled way. Nanoscale carriers of drugs provide new, exciting opportunities for smart and stimuli-responsive DDS. Such nanosized carriers do not release the payload before reaching the target and accumulate at the desired site by active or passive targeting.[6] These smart nanoscale DDS release the drug in response to various endogenous or exogenous stimuli. Temperature is the most frequently used stimulus for the diseases like inflammation and tumors. The difference in temperature between normal tissues and tumors can be efficiently utilized for triggered drug release.[7] Many clinical trials involving the combination of hyperthermia and chemotherapeutics are ongoing.

Various materials (polymers, copolymers, lipids, micelles) have been developed with thermo-responsive characteristics that had reported promising results.[8,9]

The application of mild hyperthermia in the range of 39–42°C is more effective than thermal ablation with higher temperatures > 50°C that may destroy tumor tissues.[10,11] Thermosensitive liposomes, polymeric nanoparticles, and hydrogels have been developed to release the drug at the target site in response to temperature. These synthetic polymers or lipids are developed after complex chemical reactions requiring various organic solvents.[12] Moreover, the toxicity, biocompatibility, cost, and complexity remain a challenge to the application of these systems in future clinics.[12–14] The lipids-based thermoresponsive carriers have gained significant attention in recent years after Thermodox, liposomal doxorubicin entered phase-III clinical trials with promising activity in breast cancer. However, the fabrication of these liposomes involved various complex lipids and solvents that may lead to a higher cost of therapy.[15] Cost of treatment is also a major concern in cancer chemotherapy, especially in middle- and low-income countries. The development of new, effective, and affordable cancer medicines was also highlighted at the 70th world health assembly in 2017.[16] There is a crucial need to establish new simpler, cost-effective, biocompatible, and safe carriers with temperature-responsive properties for such types of applications. We have already developed binary lipid nanoparticles for thermoresponsive drug release at 39°C. These nanoparticles were developed from natural, safe, and cheap fatty acids that melt and release the drug at a higher than normal body temperature.[17] The phase change materials, (PCMs), have gained considerable attention as thermoresponsive gating materials as they undergo reversible phase transitions over a narrow temperature range. Many researchers have utilized different types of materials that behave as PCM to release the drug in response to varying temperatures of physiological systems. Among those various polymers including polylactico-glycolic acids, polyacrylamides, and polysaccharides, tetradecanol and hexadecanol have been used in the literature for thermoresponsive characteristics.[18–21] However, the cost, compatibility, and safety of these polymers present serious concerns for formulation scientists striving to introduce advanced nanocarriers with better therapeutic efficacy, safety and affordability. Natural fatty acids are more promising phase change materials. They have advantages of safety, low cost, biocompatibility, and non-toxicity. However, the crystallization of pure fatty acids upon cooling tends to create a drug-rich outer layer and exclusion of drugs from the core. To overcome these drawbacks, the eutectic mixtures of natural fatty acids have been introduced that melt at lower temperatures than either of their component and release the drug while undergoing solid to liquid phase transition.[22] Therefore, the present study has been conceived to fabricate a novel lipid matrix based on eutectic mixtures of natural fatty acids.

In this study, we attempted to develop nanostructured lipid carriers with thermoresponsive characteristics to release the encapsulated drug at a specific temperature in solid tumors. This second generation of lipid nanoparticles utilized eutectic mixtures of fatty acids as solid lipids to alter the crystallization behavior of individual fatty acids, and to improve the drug loading capacity, release behavior, and toxicity profile. To the best of our knowledge, this is the first study to utilize eutectic mixtures of fatty acids as a novel lipid matrix for thermoresponsive lipid nano-carriers.

Materials and Methods

Materials

Myristic acid, stearic acid, span-80, polyoxyethylene (20) cetyl ether or Brij-58, $CaCl_2$, and NaCl were purchased from Sigma Aldrich (USA). Super refined oleic acid NF was obtained from Croda Inc (USA). Doxorubicin HCl was purchased from Tokyo Chemical Industry (TCI, Japan). Phosphate buffer saline, PBS, pH 7.4 was purchased from Fisher Scientific (USA). The solution of Trypan blue was purchased from Hyclone (Logan, UT). Dulbecco's modified Eagle's media (DMEM), fetal bovine serum (FBS), and penicillin-streptomycin solution were obtained from CellGro (VA, USA). CellTiter Blue cell viability assay was purchased from Promega (WI, USA). B16F10 cell line was obtained from American type culture collection (ATCC), United States.

Preparation and Analysis of PCM-Matrix

The fatty acids used as phase change materials in this study (myristic acid and stearic acid) were weighed using a high precision analytical balance (Shimadzu). A melting point apparatus was used to determine the melting point range of

individual fatty acids as well as eutectic mixtures. The samples of 20–30 mg were introduced inside a glass capillary and placed in the aluminum block with a mercury thermometer. A gradual heating mode was started, and the melting process was monitored via a built-in magnifying lens. The temperature range indicating the start and the end of the melting process was determined for each sample. A water bath with incremental temperature increase was also utilized to further confirm the results. The mean of melting points was taken and considered in this study. The eutectic mixture of pure solid fatty acids was prepared by melting and homogenous mixing of myristic acid and stearic acid at a weight ratio of 1.77:1, respectively. This eutectic mixture was cooled to room temperature and finally ground to obtain a homogenous powder. The melting point of the eutectic mixture was determined to ensure the successful preparation of the eutectic mixture of fatty acids that melt at lower temperatures than their counterparts. The crystal behavior of individual fatty acids and the eutectic mixture of fatty acids were also determined with a powder X-ray diffractometer (JDX 3532, Jeol, Japan) to check whether the eutectic mixtures suppress the crystalline behaviors of pure solid fatty acids or not. For each sample, the scanning was carried out at 2θ from 10° to 50° for 30–60 minutes. Any occurrence of chemical interaction between fatty acids during the preparation of a eutectic mixture was also studied using attenuated total reflectance Fourier transform infrared spectroscopy (Bruker, Tensor 27 Series Germany). The resolution of the instrument was set at 4 cm^{-1} with a spectral range of 7500-370 cm^{-1} (the single bounce, ATR cell equipped with a ZnSe single crystal). The spectral measurements for individual fatty acids and eutectic mixture were carried out in the range from 4000 to 650 cm^{-1} at ambient temperatures.

Preparation of PCM Based Nanocarriers

The PCM-based nanoparticles were prepared by the combined hot melt encapsulation (HME) and sonication method reported previously with slight modifications.[23] Two phases (lipid phase, aqueous phase) were prepared separately using a hot plate magnetic stirrer. The lipid phase was prepared by physical mixing of the above-prepared eutectic mixture of fatty acids and oleic acid used as a liquid lipid at a weight ratio of 6:4 to further lower the melting point of the mixture to trigger the drug delivery at a lower temperature. The lipid phase was heated at 10–15°C above the combined melting point of all lipids (41°C). Surfactant and co-surfactant solution (5%) containing Brij-58 and span-80 (3.3:1 weight ratio) was prepared in 10 mL of ultrapure water (Thermo Scientific Barnstead nanopure water purification system) heated to the same temperature as the lipid phase served as the aqueous phase. The two phases were mixed under continuous stirring at 850 rpm for 15 minutes. Finally, the dispersion was sonicated for 10 minutes and cooled down to room temperature to allow solidification of the lipid forming nanoparticles. The drug-loaded nanoparticles were prepared by adding doxorubicin (0.5 mg/mL) in the melted lipid phase. The dispersions were stored at 4°C for further analysis. The formulations were termed blank lipid nanocarriers and doxorubicin lipid nanocarriers.

Hydrodynamic Diameter and Poly-Dispersion Index (PDI)

The particle size and PDI of freshly prepared PCM-based lipid nanocarriers were analyzed using zeta sizer version 7.11 (Malvern serial number 10[illegible]336) based on the photon correlation spectroscopic principle. Briefly, the freshly prepared dispersions were 10-times diluted with ultrapure water and analyzed at 25°C, an angle of 90°, 3-scans, and 11 runs. All the measurements were done in triplicate in disposable low-volume UV-transparent disposable cuvettes with a sample volume of 50–[illegible] µL.

Zeta Potential (ZP)

The colloidal stability of nanocarriers was determined using disposable cells after 100-times dilution with ultrapure water. Briefly, the samples (1 mL) were introduced in disposable folded capillary cells (Malvern). The experimental parameters were set to 20 runs, 25°C using water as a dispersant. All the readings were taken in triplicate.

Morphology and Size Distribution

A transmission electron microscope was utilized to capture the morphology and mean size of nanoparticles. The freshly prepared samples were 10-times diluted with ultrapure water and sonicated for 1 minute. The sample of about 10–15 µL (microliter) was transferred to a piece of parafilm, and a 300-mesh carbon-coated copper grid (CF300-CU) was placed on

it. The excess sample was blotted with filter paper, washed 3 times with water, stained with 2% uranyl acetate solution, and air-dried. The transmission electron microscope (JEOL 1010) operating at an accelerated voltage of 80 kV (kilovolt) was utilized to take the microphotographs of developed formulations. The morphology and size of nanoparticles were analyzed by Image J software.

Encapsulation Efficiency (EE) and Drug Loading Capacity (LC)

The encapsulation efficiency of doxorubicin was determined by the filtration-centrifugation method using a centrifugal device. Briefly, a sample of 0.5 mL was added to the Amicon ultra 100k device (Millipore, USA) and centrifuged at 1400 g for about 10 minutes. The filtrate was analyzed for the unencapsulated drug by measuring absorbance at 480 nm with a multimode plate reader (BioTek, USA). The previously reported UV-visible spectrophotometric method after partial validation (verification) according to International council on Harmonisation, ICH guidelines was used for this purpose. % encapsulation efficiency and loading capacity were measured using an appropriate calibration curve and the following formulas:

$$\%EE = \frac{W_{total} - W_{free}}{W_{total}} \times 100 \quad (1)$$

Where W_{total} = the amount of total drug added; W_{free} = the amount of unencapsulated drug in filtrate analyzed:

$$\%LC = \frac{W_{encapsulated\ drug}}{W_{total\ lipids}} \times 1 \quad (2)$$

The measurements were carried out in triplicates.[25]

Fourier-Transform Infrared (FTIR) Spectroscopy

The encapsulation of drug in lipid matrix as well as the interaction between drug and lipid matrix was analyzed by Fourier transform infrared (FTIR) spectrometer (Bruker, Tensor 27 Series Germany). The free drug, equimolar physical mixture of excipients and doxorubicin and doxorubicin lipid nanocarriers was analyzed by recording the spectrum in the range 4000–650 cm^{-1}. Any occurrence of physicochemical interaction among the excipients and drug during the preparation process was identified by characteristic peak shifts or modifications.

Drug Release

The dissolution studies were carried out to surrogate the release behavior of doxorubicin from optimized lipid nanocarriers and aqueous solution of using the dialysis bag method. United States Pharmacopeia (USP) type II dissolution apparatus (Pharma Test, Hamburg, Germany) with paddle assembly was employed for this purpose.[26] The instrument was set at a speed of 50 rpm, temperature (37°C, 41°C, 43°C), and filled with 450 mL of release media (Phosphate buffer saline PBS pH 7.4 and 6.8). A dispersion equivalent to 1 mg of doxorubicin was added to the cellulose ester dialysis membrane (MWCO 14 kDa) and immersed in media. An aqueous solution of doxorubicin (free doxorubicin) was also checked similarly. Samples of 2 mL were taken at predetermined time intervals and replaced with the same amount to maintain sink conditions. The samples were filtered and centrifuged to separate unencapsulated drug by using a centrifugal device as described previously. The free drug absorbance was taken with a UV-visible spectrophotometer (IR, SECO, U2020, Schwarzenbek, Germany) at 480 nm and fitted to a standard calibration curve of doxorubicin. The amount of drug and cumulative percentage of doxorubicin released at different time points was calculated. The reproducibility, linearity, and accuracy of the spectrophotometric method were evaluated according to ICH guidelines.[27] Each sample during the study was measured in triplicate.

Analysis of Drug Release Kinetics

The mechanism of drug release was exploited using the drug dissolution, DD Solver Excel add-in. The experimental data obtained from drug release experiments were fitted to different kinetics models (zero-order, first-order, Higuchi, Korsmeyer-Peppas, Hixson Crowell and Weibull model). The best-fitting kinetic model was selected based on the

highest R^2-value obtained. The value of the diffusional release exponent "n" was calculated to determine the mechanism of drug release.

Stability Studies

The stability studies were carried out by storing the selected formulations (based on the smaller size with better monodispersion) at 4°C for 14 days period. The size distribution, zeta potential, and entrapment efficiencies were checked on day-0, day-7, and day-14.[28,29] The statistical analysis for comparison of parameters at different time intervals was carried out by Student's *t*-test. The results were considered significant for $p < 0.05$.

Biological Assays

Cell Culture

Murine melanoma, B16F10 cells were cultured in Dulbecco's Modified Eagle's Medium (DME), modified to contain 4 mM L-glutamine, 4500 mg/L glucose, 1 mM sodium pyruvate, and 1500 mg/L sodium bicarbonate. The medium was supplemented with fetal bovine serum, FBS (10%), and antibiotics (100 U/mL Streptomycin). The cells were regularly checked for change of media and passaged twice per week.

Cell Viability Determination

Upon reaching 70% confluency, cells were detached with trypsin and counted via a dead cell staining assay using Trypan Blue. Briefly, cell suspensions were diluted four times with Trypan Blue solution, blue staining of dead cells. The number of viable or live (seen as bright cells) was counted using a bright-line hemacytometer (Hausser Scientific) specifically designed for cell counts. Cell suspension volume was calculated to contain a required number of cells and diluted with the medium. Cells were seeded at a density of 7×10^3 cells/well of a 96-well plate and incubated overnight at 37°C and 5% CO_2. The cells were treated with doxorubicin solution from 0.125 to 2 µg/mL as well as blank lipid nanocarriers to evaluate the cytotoxicity of the free drug and carrier, respectively. The optimized formulation (UT-2) of the developed thermoresponsive lipid nanocarriers was also tested at concentrations from 0.5 to 2 µg/mL of loaded doxorubicin. The treated cells incubated at 37°C for 24 hours were termed as a control for comparison of cytotoxicity at two different temperatures. The treated cells were kept in an incubator set at 41°C for 1 hour and then incubated for 24 hours at 37°C in a cell incubator. At the end of the incubation period, the viability of adherent cells was checked with Cell Titer-Blue® assay (Promega, Madison, USA) according to the manufacturer's protocol. A graph between percent viability and drug concentration was plotted to determine the dose-response relationship.

Biosafety Determination

Hemocompatibility Assay

The hemolysis potential of blank, as well as the loaded carriers, was determined using a previously published protocol with slight modifications. First, a saline solution was prepared by mixing 55.5 mg of $CaCl_2$ and 425 mg of NaCl in 50 mL of ultrapure water with subsequent filtration carried out to remove any insoluble material. Fresh blood was collected from immunocompromised mice and added to the tubes with an anticoagulant. The erythrocytes were separated after centrifugation at 500xg for 5 minutes and washed with 1 mL of saline solution. The supernatant was discarded, and the pellet was washed with saline three times more. The erythrocyte solution, 2% v/v in saline solution was prepared and utilized within 24-hours. The assay was performed using two 96-well round-bottom microwell plates. Different concentrations of blank and drug-loaded lipid nanocarriers in saline solution ranging from 250 to 2000 µg/mL of total lipid concentration were added. A negative control (saline solution) and positive control (2% Triton-x-100 in saline solution) were also added to both plates. The erythrocyte solution, 100 µL, was added to each well in one plate, while a second plate was left blank to null any color or turbidity that might interfere with the absorbance measurements. The plate was incubated for 60 minutes at 37°C along with slight agitation followed by centrifugation. (500 ×g, 10 minutes). The supernatant was transferred to another plate for measurement of released hemoglobin by taking absorbance value at 540 nm. The data were expressed as percent hemolysis for different concentrations of blank and loaded lipid nanocarriers.[30,31]

Acute Toxicity Studies

Animals

Male albino rats (9–11 weeks old) were obtained from the Pharmacy Department of Bahauddin Zakariya University, Multan, Pakistan. All the animals were analyzed carefully before transfer to the animal house of the Faculty of Pharmacy, the Islamia University Bahawalpur, Railway Campus, Pakistan. All the studies were approved by the Pharmacy Animal Ethics Committee (PAEC) of the Islamia University Bahawalpur, Pakistan (Ref. No.22-2020/PAEC). The study procedures and protocols were adopted in compliance with the Organization for Economic Co-operation and Development Guidelines for Testing of Chemicals, 2001.[32] The animals were kept in clean cages for one week in a controlled temperature and humidity environment. The animals were exposed to light and dark cycles (12/12 hr.) with free access to a standard diet and drinking water. They were divided randomly into three groups (four animals per group) and marked clearly to differentiate among groups. The animals were acclimatized to the conditions of the animal house before dosing. On the seventh day, animals were fasted overnight for food only however water was not stopped. The rats were weighed individually before administration of testing substances. All the animals were treated in compliance with protocols approved by PAEC, IUB for this study.

Dose Preparation and Administration

All the doses were prepared fresh on the day of use. The animals in Group-I were dosed with 1.5 mL of normal saline as control. Group-II animals were treated with 1.5 mL of blank lipid nano-carriers at 50 mg/100 g of body weight. Group-III animals were treated with 1.5 mL of lipid nano-carriers with similar composition as for Group-II except also containing doxorubicin at 1 mg/100 g of body weight. The animals were provided with free access to standard food and water as before, 3 hours after dosing's completion. All the animals were critically observed for an additional two hours continuously after dosing for any type of allergic reaction, shock, or mortality. The animals were monitored carefully for food and water intake, behavioral change, weight loss, diarrhea, convulsions, lethargy, or coma. The same was carried out periodically over the next 14-days period. After the end of the treatment duration, animals were reweighed. All the animals were anesthetized using a mixture of ketamine and xylocaine injection with doses of 80 mg/kg and 15 mg/kg respectively.[33] Blood samples were collected by capillary tubes after retro-orbital puncture and immediately transferred to serum separator tubes with a yellow top and EDTA (ethylenediaminetetraacetic acid) tubes with a pink top. Plasma and serum were collected for hematological and biochemical parameter analysis. Anesthetized animals were sacrificed to retrieve the heart, liver, spleen, and kidney for histopathological studies. The organs were kept in formalin solution (10% v/v). The slices were sliced and stained to fix over slides for further microscopic examination.

Statistical Analysis

All the data were analyzed using GraphPad Prism 8.4.3. The Student's *t*-test, one-way or two-way analysis of variance (ANOVA) with Tukey's multiple comparison test was applied depending upon the type of groups to be compared to determine the statistical significance of differences between means. The p-value less than 0.05 was considered significant and denoted as ≤0.05 as *, ≤0.01 as **, and ≤0.001 as ***.

Results and Discussion

Analysis of PCM-Matrix

This study reports the preparation of eutectic mixture (UM) of natural fatty acids that are safe, cheap, scalable, stable, and biodegradable alternatives to various excipients being utilized for stimuli-responsive drug delivery systems. The eutectic mixtures are defined as the combination of two or more compounds that do not react with each other to form a new compound when mixed in a particular ratio however the mixture melting point is lower than the individual components.[35,36] The eutectic mixture (1.77:1 weight ratio) of myristic acid and stearic acid started to melt at 44.2°C which is lower than the individual melting points of the fatty acids (53 and 69°C respectively) observed by two different laboratory-scale methods. The weight ratio selected, and corresponding melting point was observed in available literature.[37] This observation confirmed the successful fabrication of a UM of fatty acids that exhibited significant melting point depression when compared to pure fatty acids. A similar finding was recently reported in a study for the use of a UM of lauric acid and stearic

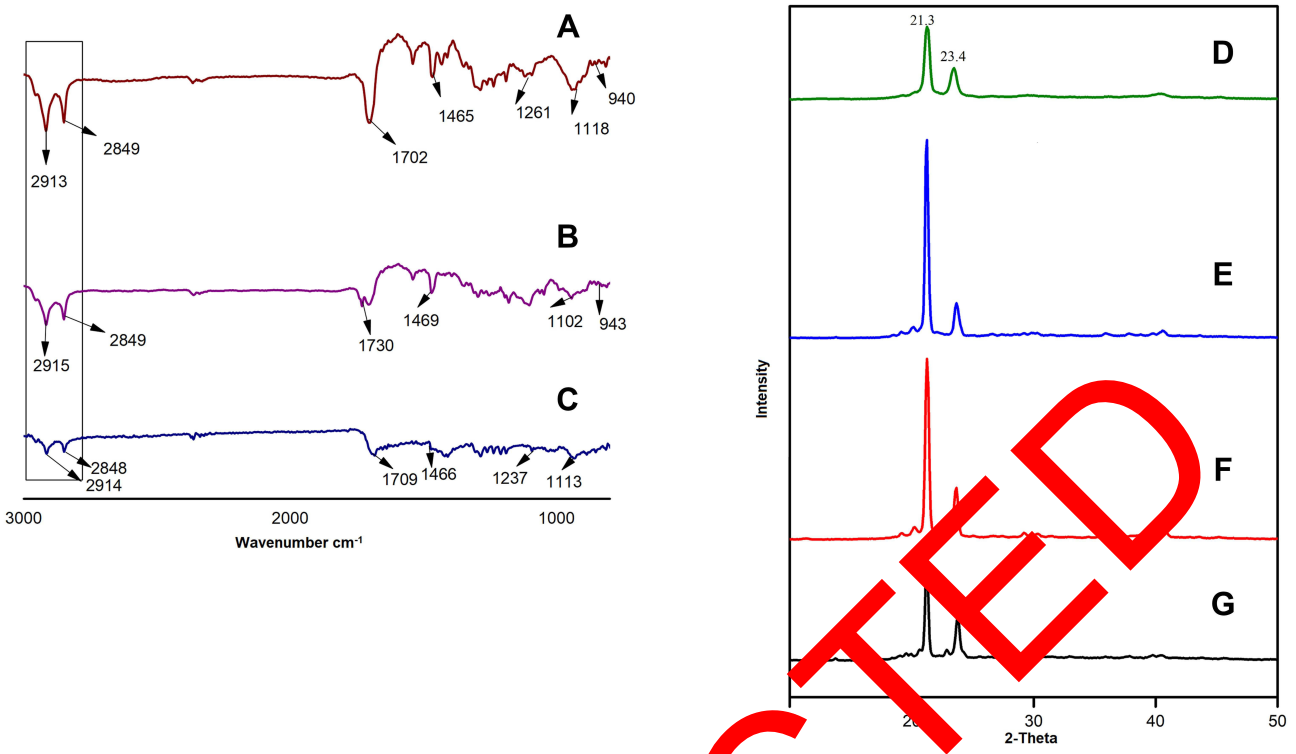

Figure 1 (**A**) FTIR spectroscopic analysis of eutectic mixture of myristic and stearic acid. (**B**) FTIR spectroscopic analysis of stearic acid. (**C**) FTIR spectroscopic analysis of myristic acid. (**D**) P-XRD patterns of eutectic mixture of myristic acid and stearic acid. (**E**) P-XRD patterns of physical mixture of myristic acid and stearic acid. (**F**) P-XRD patterns of stearic acid. (**G**) P-XRD patterns of myristic acid. All data were presented as mean ± S.D (n=3).
Abbreviations: FTIR, Fourier transform infrared; P-XRD, powdered x-ray diffraction.

acid as a thermo-responsive gating material. This study reported the single peaked melting behavior of the eutectic mixture at 39°C which was less than both individual melting points of fatty acids (44 and 69°C) respectively.[38]

Powder X-ray diffraction (P-XRD) patterns were analyzed to assess the crystal behavior of individual fatty acids and their eutectic mixtures to achieve improved drug loading objectives for cancer cells killing.[39] P-XRD peaks of individual fatty acids (Figure 1F and G) and the eutectic mixture of those (Figure 1D) were plotted to compare the crystallinity of both samples. The decreased intensity of characteristic peaks at 21.3° and 23.4° indicated that the crystal behavior of the UM was reduced to some extent. These results were further supported by taking a mixture of the same fatty acids mixed without a eutectic ratio (1:1) that produced more intensive peaks as compared to the UM reflecting a less ordered structure of the lipid matrix[40] (Figure 1E). The physicochemical interaction such as the formation of any new bonds between fatty acids was determined by analyzing the absence of characteristic peaks, presence of new peaks, or peak shifts.[41] The peaks analysis of the FTIR spectrum revealed that there was no chemical interaction between fatty acids when mixed in a eutectic ratio. The individual fatty acids (Figure 1B and C) and UM (Figure 1A) exhibited similar characteristic peaks with the appearance of absorption bands at the same time that confirmed the compatibility between excipients and successful fusion. The intact peaks of stearic acid (Figure 1B) and myristic acid (Figure 1C) were associated with C-H stretching vibrations at 2913 and 2849 cm^{-1}, C=O stretching vibrations at 1702, C-H bending vibrations at 1465, C-O stretching vibrations, at 1261, and O-H bending vibrations at 940 cm^{-1} were found in a eutectic mixture of fatty acids (Figure 1A).[42,43] This study unveiled the capability of eutectic mixture of fatty acids to act as a phase change material after solid-liquid phase transition for on-demand drug release application.

Preparation of Lipid Nanocarriers

The lipid nanocarriers were produced by the combined HME and sonication method developed and reported previously with slight modifications.[44] The combination of methods was employed to achieve critical control over the texture and homogeneity of the final formulation. The particle size in this method is forced to reduce by applying

shear force, cavitation, and the collision of particles.[45] The reported method has been found to be simple, bypassing the extensive utilization of expensive organic solvents at various steps, and hence found to be scalable. The methods like solvent emulsification and solvent injection involve the use of toxic organic solvents that impacts the quality and biosafety of developed nanocarriers. The probe sonication method has been extensively employed; however the metal contamination imparted is a serious limitation.[46] In comparison, our method was simple, safe, and easily adaptable. The lipid phase consists of eutectic mixture (myristic acid and stearic acid) as solid lipid and oleic acid (6:1) as liquid lipid. The amount of liquid lipid added served to suppress the corresponding melting point of the lipid matrix (39.9–41.3°C) to achieve mild hyperthermia-assisted drug release with minimal harm to cells themselves.[47] The drug was encapsulated in the lipid matrix due to ion-pairing with oleic acid.[48] The process and excipient variables were optimized for this study to achieve passive targeting via enhanced permeability and retention effect (Table 1). Three lipid concentrations and three surfactant concentrations affecting physicochemical characteristics were tested in this study. These concentrations were selected based on various formulation development trials to achieve the desired characteristics for the proposed study. The total lipid concentration was varied but the ratio of liquid lipid to the UM of solid fatty acids was kept constant to keep the same melting behavior of the lipid construct. The ratio of surfactant and co-surfactant was also kept the same, and total surfactant concentration was varied in this study.

Size Distribution and PDI

The particles' size and their distributions are very important to depict the stability and in-vivo behavior of final formulations. The narrow distribution and nanometric size of carriers are critical parameters for achieving enhanced permeability and retention (EPR) effect-based targeting during cancer treatment.[49] The dynamic light scattering technique and zeta sizer software was utilized to determine the intensity of scattered light that demonstrated a hydrodynamic diameter with a hydration shell around the particles. The average hydrodynamic diameter and PDI of all five developed formulations ranged from 94.59–219.3 nm and 0.160–0.479 as described in Table 1. The narrow size distribution of the optimized formulation confirmed the development of a monodispersed system with a PDI < 0.3 which is desirable for targeted tumor therapy. Nanocarriers with a size less than 400 nm are required to achieve EPR effect; however, nanocarriers of size less than 200 nm are required for prolonged circulation.[49] The increasing concentration of surfactant has been reported to efficiently reduce the interfacial tension and particle size. This effect was noted when the concentration of surfactant was increased from 3% to 5% and the resulting particle size was decreased from 195.9 to 94.59. All developed formulations were optimized based on size distribution and stability. The optimized formulation (UT-2) was selected with the least variation in size distribution, zeta potential, and encapsulation efficiency before and after 14 days of storage at 4°C. The size distribution by the intensity of the optimized formulation, UT-2, is presented in Figure 2. The results were acquired from Malvern Instrument Report.

Table 1 The Composition, Mean Particle Size, Polydispersity Index, Zeta Potential, Percent Encapsulation Efficiency, and Loading Capacity of Developed Formulations

Formulation Code	Amount of Lipid (mg)	Concentration of Surfactants (%)	Particle Size (nm)	PDI	Zeta Potential (mV)	EE (%)	LC (%)
UT-1	80	3	195.9±7.56	0.479±0.15	−32.0±3.51	63.3±2.07	3.96±0.13
UT-2	80	4	172.9±4.92	0.160±0.01	−26.7±2.94	68.16±1.51	4.23±0.12
UT-3	80	5	94.59±5.22	0.132±0.03	−22.7±2.15	69.7±0.53	4.35±0.04
UT-4	90	4	205.0±10.19	0.330±0.19	−25.2±3.73	72.3±0.67	4.03±0.04
UT-5	100	4	219.3±8.65	0.401±0.16	−25.6±2.50	71.9±0.45	3.60±0.03
Blank	80	4	170.0±6.58	0.186±0.06	−27.3±3.10	-	-

Note: Data are presented as mean ± SD (n=3).
Abbreviations: mg, milligram; nm, nanometer; PDI, polydispersion index; mV, millivolt; EE, encapsulation efficiency; LC, loading capacity.

		Size (d.nm):	% Intensity:	St Dev (d.nm):
Z-Average (d.nm): 172.9	Peak 1:	201.0	100.0	72.67
PdI: 0.160	Peak 2:	0.000	0.0	0.000
Intercept: 0.930	Peak 3:	0.000	0.0	0.000
Result quality : Good				

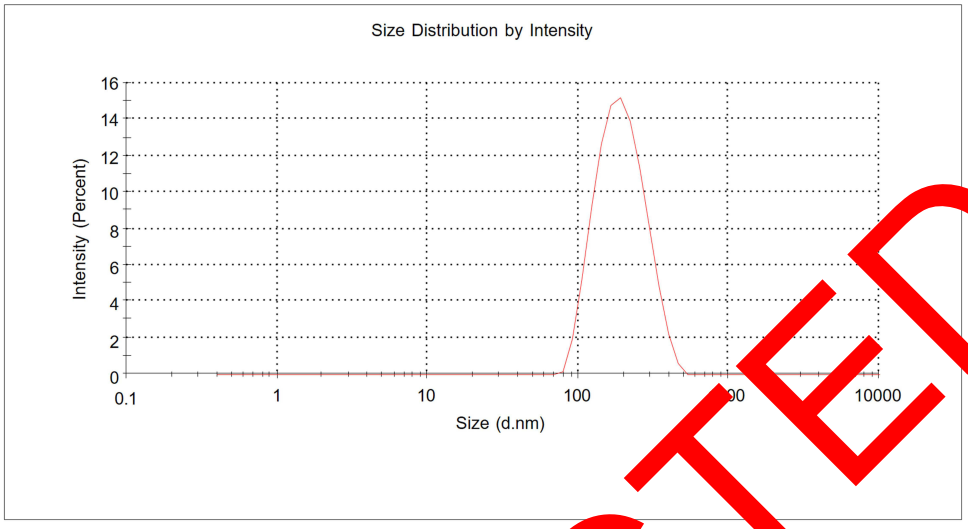

Figure 2 The particle size distribution by the intensity of optimized formulation characterized by dynamic light scattering technique.
Abbreviations: Z-average, intensity weighted mean hydrodynamic size; d.nm, diameter value in nanometer; PdI, polydispersity index.

Zeta Potential/Electrokinetic Potential

An optimum zeta potential value is a critical parameter to determine the colloidal stability of nanostructured lipid carriers. The value of zeta potential provides information about the surface charge of particles and physical stability acquired during shelf life.[50] The zeta potential was determined by the electrophoretic mobility method to determine the colloidal stability of prepared lipid nanocarriers. The steric stabilization of nanoparticles requires a minimum zeta potential of ± 20 mV[51] and highly stable liposomal formulations exhibit zeta potential values > ± 30 mV.[52] In our study, all the developed formulations were having zeta potential in the range of −22.7 to −32 mv that show excellent colloidal stability required during shelf life. We utilized nonionic surfactants to stabilize our system which had been reported to

		Mean (mV)	Area (%)	St Dev (mV)
Zeta Potential (mV): -26.7	Peak 1:	-26.7	100.0	7.08
Zeta Deviation (mV): 7.08	Peak 2:	0.00	0.0	0.00
Conductivity (mS/cm): 0.00266	Peak 3:	0.00	0.0	0.00
Result quality : Good				

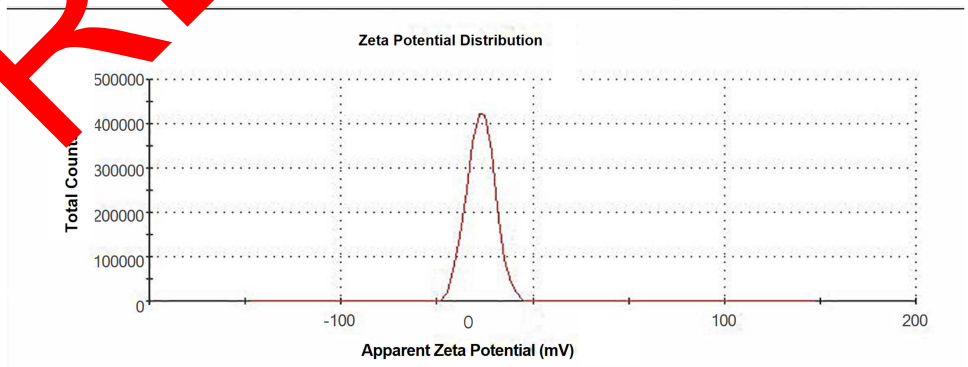

Figure 3 Zeta potential distribution of optimized formulation characterized using electrophoretic mobility technique.
Abbreviations: mv, millivolt; mS/cm, millisiemens per centimeter.

reduce the size and surface area of particles by masking the surfaces.[53] The value of zeta potential was negative and lowered with increasing surfactant concentration as depicted in Table 1. The concentration of non-ionic surfactant was found to lower the value of zeta potential as reported by various other researchers.[54] The non-ionic surfactants tend to shift the shear plane of particles resulting in a lowering of zeta potential.[25] The zeta potential distributions of optimized formulation, UT-2 are given in Figure 3.

Encapsulation Efficiency and Drug Loading Capacity

The solubility of the encapsulated drug in a lipid matrix, types and amount of surfactants, solid and liquid lipids utilized, and various processing variables have been reported to affect the encapsulation efficiency and drug loading capacity.[55] Doxorubicin being a water-soluble drug has a low affinity for lipids and alternative strategies have been proposed to achieve better EE for therapeutic purposes. Lipophilic anions such as oleic acid have been propo improve the EE of doxorubicin in lipid nanocarriers.[56] The encapsulation efficiency of all developed formulation was analyz by UV-visible spectroscopy method at wavelength 480 nm (method validation data given in Supplementary Figure 1 and Supplementary Table 1). The encapsulation efficiency of all the formulations was found in the rang of 63.9– 3% (T le 1). The EE increased when the concentration of lipid was increased, probably due to increas lipid a ilable old the drug. The increased viscosity of the system did not allow the diffusion of the drug molecule to th outer phase. Second-generation lipid nanoparticles were reported to encapsulate more drugs with less expul on due t e adde iquid lipid.[57] The liquid lipid (oleic acid) used in this study was also reported to increase the en ap lation effic of doxorubicin due to ion-pairing potential.[58] Furthermore, the UM of fatty acids also affected the encapsu ion efficiency as reported in literature.[38] All these possible explanations might influence the high encapsu efficiency o oxorubicin within lipid nanocarriers.

Transmission Electron Microscopy (TEM)

The TEM photomicrographs of the optimized formulation were en at nification (direct magnification) and voltage of 30,000 × and 80 kV, respectively. The images (Fi re easonably highlight the presence of spherical particles (size ranging from 80 to 110 nm) with a dense core that may be h erog eous as reported in literature.[59] The particle size data obtained from DLS, and TEM are usuall ent be use DLS is a light scattering intensity-based technique while TEM gives a number average diame . The ndersiz results obtained by TEM may be due to the absence of

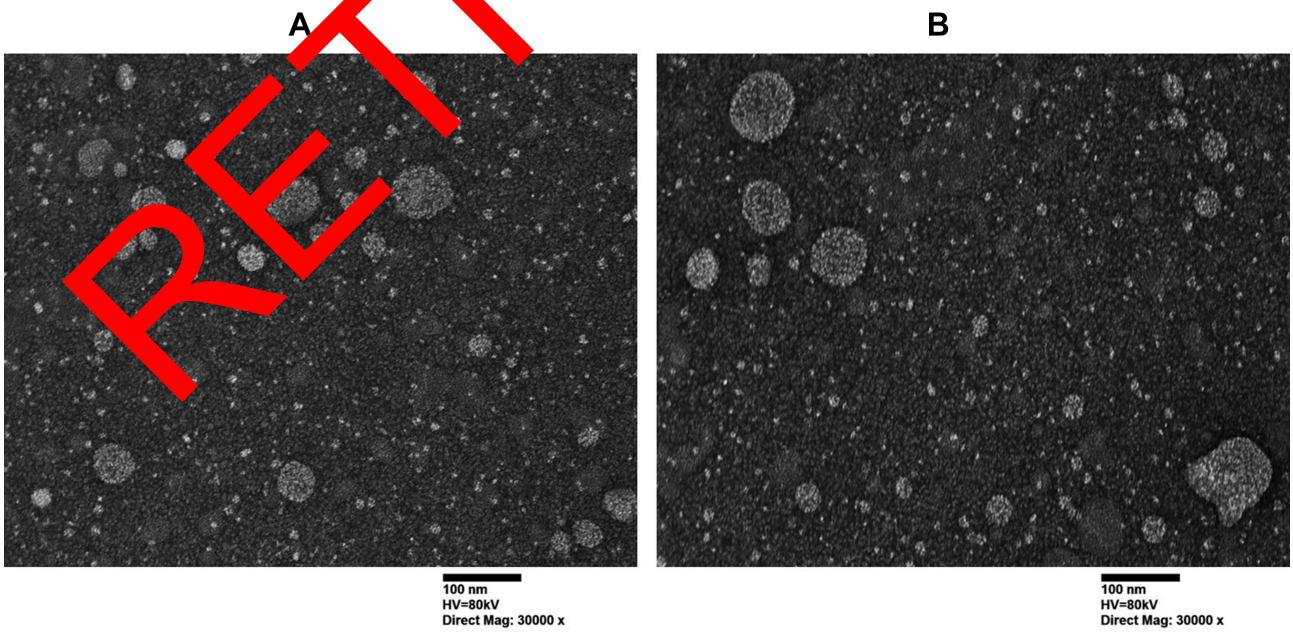

Figure 4 Transmission electron microscopic image of (**A**) blank lipid nanocarriers and (**B**) doxorubicin lipid nanocarriers. The scale bar is 100 nm.
Abbreviations: nm, nanometer; kV, kilovolt; HV, high voltage.

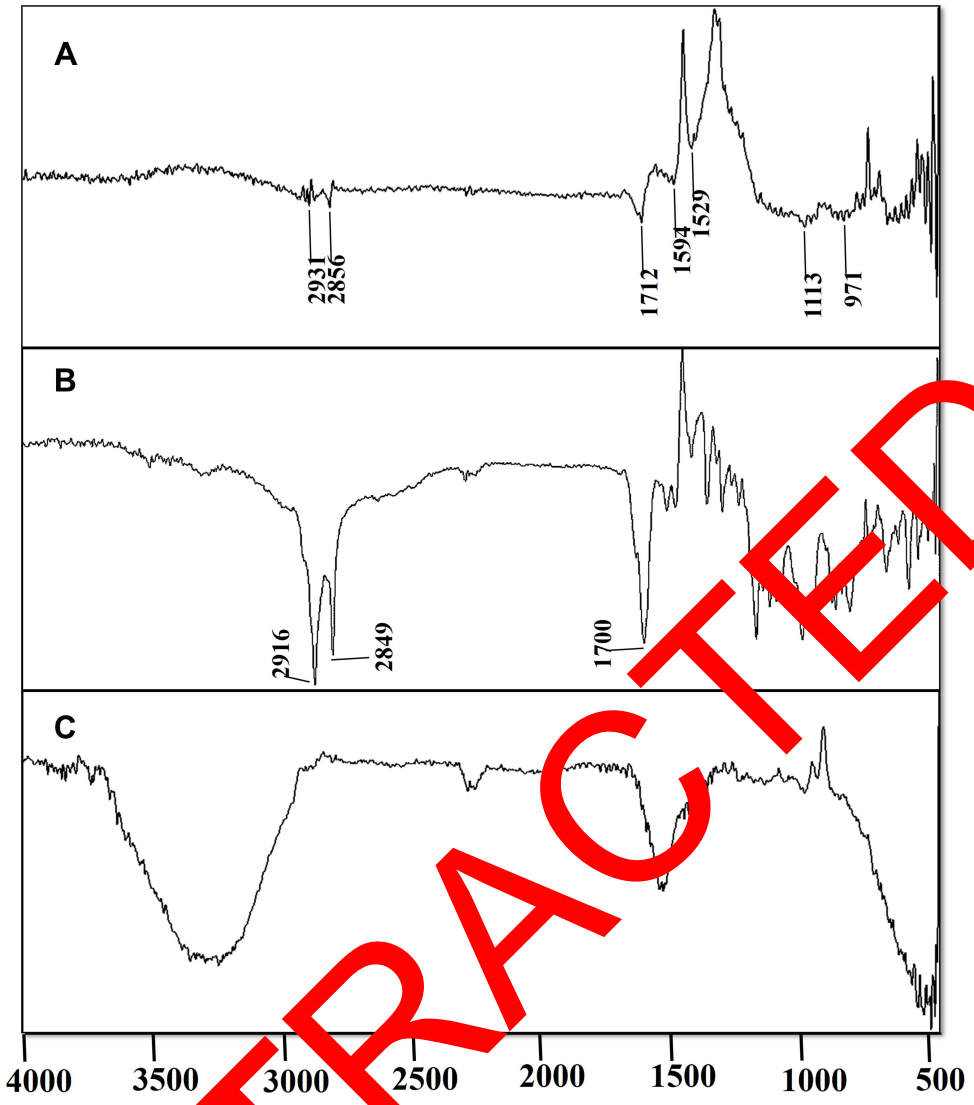

Figure 5 FTIR spectrum of (**A**) doxorubicin, (**B**) physical mixture of doxorubicin and excipients (**C**) doxorubicin lipid nanocarriers.

a hydration layer around the particles after drying.[52] The discrepancy in size measured by the two different techniques has also been reported by others.[60,61]

Fourier-Transform Infrared Spectroscopic Analysis

FTIR spectra of doxorubicin-loaded lipid nanocarriers (Figure 5C), physical mixture of doxorubicin and excipients (Figure 5B), and pure doxorubicin drug (Figure 5A) were recorded. For doxorubicin, the characteristic peaks found at 2931 and 2856 cm^{-1} were attributed to -CH stretching of alkanes, 1712 cm^{-1} (C=O) 1594 cm^{-1} (phenol ring), 1529 cm^{-1} (aromatic ring), 1113 cm^{-1} (C-O tertiary alcoholic groups), 971 cm^{-1} (C-O) were in agreement with previous data.[62–64] The physical mixture of drug and excipients represented major characteristic peaks with increased intensity at 2916, 2849, and 1700 cm^{-1} due to symmetric and asymmetric CH_2 stretch and stretching vibration of C=O in fatty acids (oleic acid).[65] The lipid nanocarriers loaded with doxorubicin did not show intensive peaks of doxorubicin perhaps due to the small quantity of doxorubicin added or low sensitivity of FTIR spectroscopy. The disappearance of peaks shows that the drug was encapsulated in the inner core or lipid matrix as the major characteristic bands were buried. Similar findings were reported in literature.[66,67]

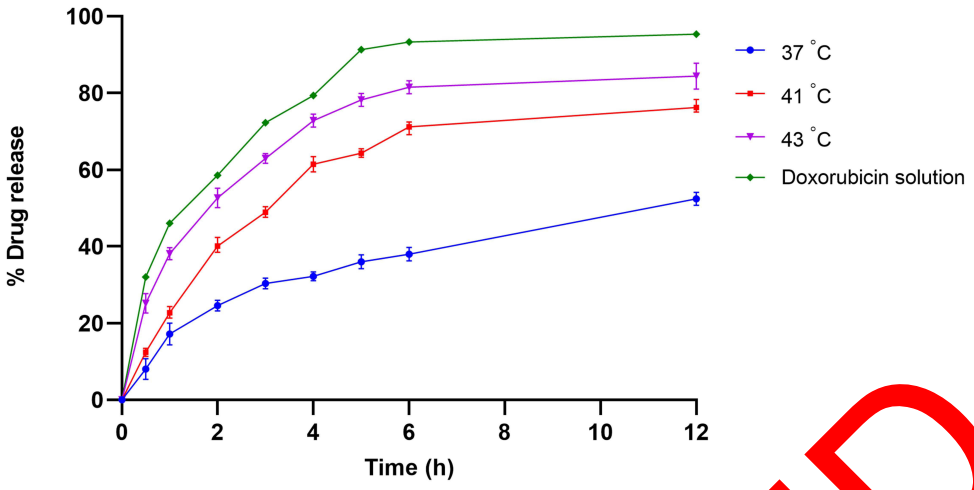

Figure 6 The release profile (12-hours) of doxorubicin from optimized formulation and aqueous solution at temperatures 37 °C, 41°C, and 43°C in release media having pH 6.8. Data are presented as mean± SD.

Temperature-Responsive Drug Release Analysis

The release of the drug from lipid nanocarriers was checked for up to 12 hours at three different temperatures (37°C, 41°C, and 43°C) and pH 6.8 during this study (Figure 6). The drug release was also assessed at a slightly basic pH of 7.4 and 6.8 for up to 48 hours as presented in the supplementary material (Supplementary Figure 2). The release of drugs from lipid nanocarriers was compared with drug release from an aqueous solution of doxorubicin (free doxorubicin). The proper sink conditions were ensured throughout the experiment to solubilize all the drug that was released into the media. The aim of preparing phase change lipid nanocarriers was to offer abrupt drug release in response to hyperthermia. We have compared the release of drugs from lipid nanocarriers at 37, 41, and 43°C. The release of drug from lipid nanocarriers at 37°C represents a model condition for formulation of doxorubicin-loaded fatty acids-based lipid nanocarriers reported previously.[56,68] Then the model doxorubicin release profile was compared with our innovative thermo-responsive drug release at 41°C and 43°C. It was observed that at all temperatures, the release of the drug was sustained for more than 24 hours. The conventional lipid nanoparticles have been reported to prolong the drug release up to 48 hours.[69] At 37 °C, the drug release from a doxorubicin aqueous solution was about 55% within the first two hours. However, the release of doxorubicin from the nanocarriers was less than 20% during that time. This was expected because the drug molecules from the aqueous solution escaped easily without any hindrance from the dialysis membrane (MWCO 14 kDa) and had excellent solubility in the release media.

The release of drug from nanocarriers was slow as compared to the free drug because it required a mechanism (erosion, desorption, disintegration) that takes more time to release the drug.[70] The release behavior also shows that the temperature has a prominent effect because an abrupt release at 41 and 43°C was observed. This might happen due to the melting of lipid construct and the release of payload above the melting range. These findings support the conclusion that drug release can be controlled by temperature and temporal regulation can be achieved. A similar temperature-dependent release behavior was reported by Xu et al, from thermoresponsive copolymer nanoparticles.[71] The amount of drug release was higher at a slightly acidic pH probably due to increased protonation and solubility of doxorubicin at lower pH as compared to a slightly basic pH of 7.4 (Supplementary Figure 2).[72] The tumor microenvironment is slightly acidic and faster release will occur due to decrease ion-pairing interactions and a decreased log D value of doxorubicin favoring its partition into the aqueous phase. This effect was observed by Lages et al for 21% doxorubicin release from nanostructured lipid carriers at pH 7.4 for up to 24-hours as compared to 39% release at 6.8 pH.[73]

Drug Release Kinetics

A suitable fitting of drug release kinetics data is very important for proper modeling to find out the appropriateness of drug accumulation and in-silico simulation of fast drug delivery in tumors using thermally triggered nanocarriers. The drug release parameters for zero order, first order, Higuchi model, Korsmeyer-Peppas model, Hixson-Crowell model and Weibull model are presented in Table 2. The release behavior of DOX from PCM-based nanocarriers presented two different models as a function of temperature. At 37°C, the highest value of R^2 was achieved with Korsmeyer-Peppas model and Weibull model with n-value of 0.472. At 41 and 43°C the highest value of R^2 was achieved with the Weibull model and n-value of 0.379 depicting Fickian diffusion based drug release mechanism.[74] The Weibull model has been extensively applied as an empirical model of triggered and extended-release data. Lu et al described that the temperature-responsive drug release from thermoresponsive liposomes was hardly fitted by the commonly used models for zero order, first order, and Higuchi model. However, this type of release demonstrated a good fit with both Korsmeyer-Peppas and Weibull models[75] which demonstrated good agreements with these findings. The drug release data were fitted to various kinetic models using DD-solver Excel add-in as shown in Table 2. The highest value of R^2 was achieved with the Weibull model and Korsmeyer-Peppas model with an "n" value less than 0.5 showing the classical Fickian diffusion-controlled mechanism (Table 2). This mechanism of doxorubicin release from nanostructured lipid carriers has been reported by various research groups.[76,77] The best-fitting curve of kinetic modeling data using the Weibull model is presented in Figure 7A–C. The kinetic modeling of dissolution parameters at three different temperature conditions (37, 41 and 43°C) and pH 6.8 using zero-order, first-order, Higuchi, and Korsmeyer-Peppas mathematical model was also carried out and fitted curves have been represented in the supplementary material (Supplementary Figures 3A–C, 4A–C, 5A–C, and 6A–C).

Stability Study

The selected formulations (UT-2 and UT-3) were analyzed for particle size, zeta potential, and encapsulation efficiency at selected time intervals. It was found that there was no visual change in the clarity of UT-2. The particle size (193.4±5.65), zeta potential (−22.0± 0.55), and percent encapsulation efficiency (91.4±2.9) of UT-2 after a 14-days period did not change

Table 2 In-vitro Dissolution Parameters of Optimized Formulation (UT-2) at pH 6.8

Kinetic Model	Parameters	Temperature (°C)		
		37	41	43
Zero order	K_0	5.680	9.090	11.580
	R^2	0.580	0.400	0.250
First order	K_1	0.080	0.210	0.360
	R^2	0.830	0.940	0.970
Higuchi	K_H	15.860	25.90	33.240
	R^2	0.980	0.920	0.930
Korsmeyer-Peppas	K_{KP}	16.650	29.210	40.950
	R^2	0.990	0.935	0.975
	n	0.472	0.431	0.379
Hixson Crowell	K_{HC}	0.025	0.060	0.096
	R^2	0.765	0.887	0.951
Weibull	R^2	0.993	0.983	0.995

Abbreviations: K0, zero order model release constantL; R^2, regression co-efficient; K1, first order model release constant; K_H, Higuchi model release constant; K_{KP} Korsmeyer-Peppas model release constant; n, release exponent; KHC, Hixson Crowell release constant.

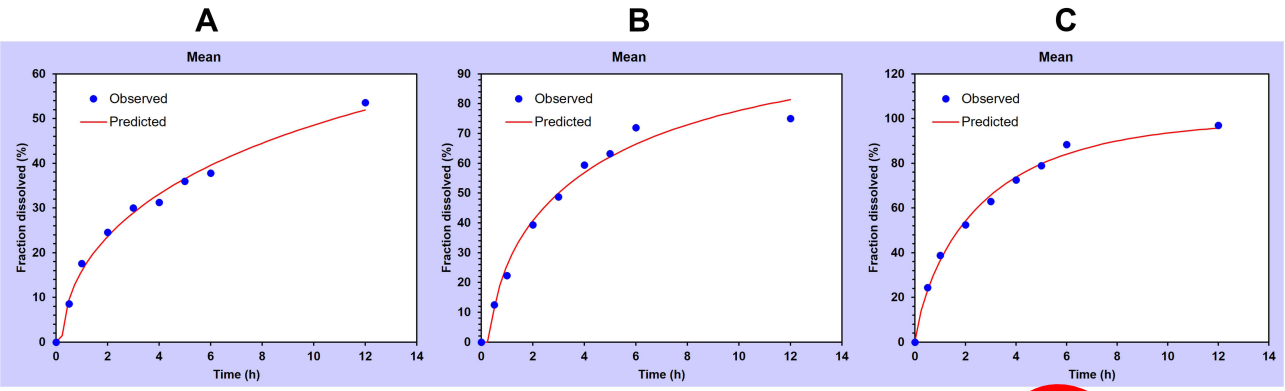

Figure 7 Dissolution data modeling of Weibull model at (**A**) 37°C, (**B**) 41°C (**C**) 43°C and pH 6.8.

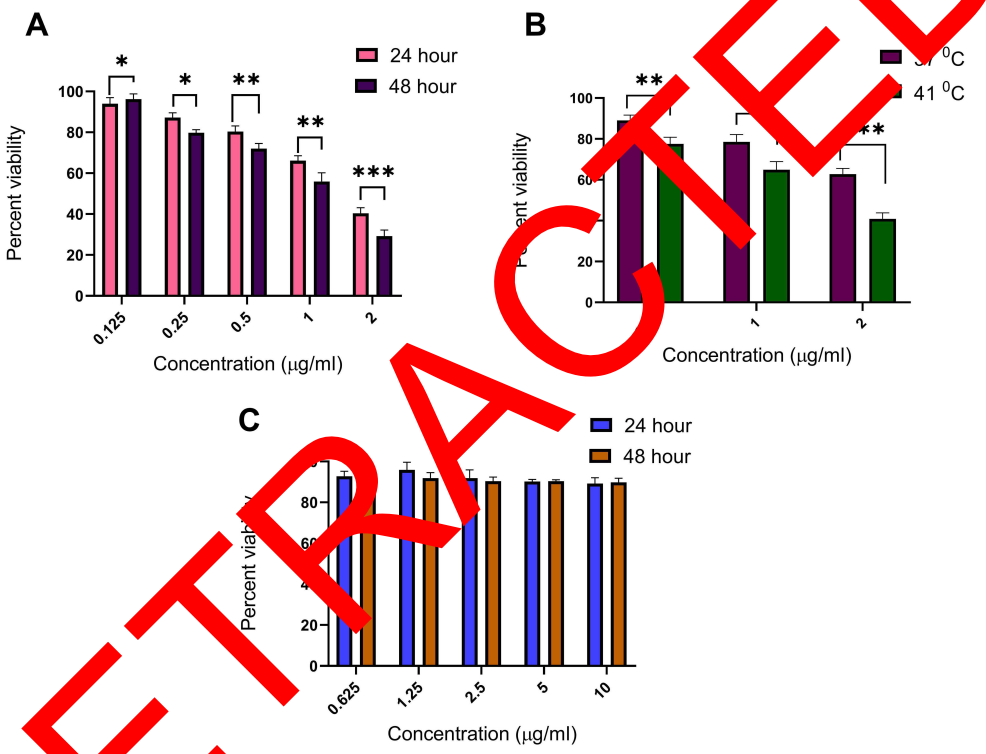

Figure 8 The p bility i nonolay f B16F10 cells characterized using cell titer blue assay treated with (**A**) free DOX at varying concentrations and incubation periods (**B**) d orubicin id nanoca varying concentrations of doxorubicin incubated at 37°C for 24 hours and with 1 hour at 41°C followed by 24 hours at 37°C, and (**C**) b lipid nano riers at var g concentrations and incubation periods. Data are presented as mean ± SD, n=3, *p < 0.05, **p ≤ 0.01, ***p ≤ 0.001.

significantly. he size distribution of UT-3 after a 14-days period was (243.6±8.91) with zeta potential value (−14.7±0.94) and encapsulation efficiency (59.95±3.6). The surfactant concentrations had a critical role in the stability and percent encapsulation efficiency. An optimum concentration of surfactant is necessary to cover nanoparticles' surfaces, retention of drugs within nanocarriers, and prevent coalescence.[28] The findings of this study suggested that lipid nanocarriers were stable during storage.

In-vitro Cytotoxicity Assay of Doxorubicin Lipid Nanocarriers

The cytotoxicity of the free drug and blank lipid nanocarriers on B16F10 cells was evaluated after 24- and 48-hour incubation periods. As depicted in Figure 8A, a clear dose-response relationship was found at concentrations of 0.125–2 µg/mL that were more significant at 0.5–2 µg/mL. The blank lipid nanocarriers depicted more than 90% cell viability at

studied concentrations and incubation periods (Figure 8C). The lipid nanocarriers with 0.5–2 µg/mL doxorubicin concentrations were tested in this study (Figure 8B). The cytotoxicity of doxorubicin-loaded lipid nanocarriers with incubation at 41°C for one hour and further incubation at 37°C was followed to minimize the impact of temperature on cells. As previously described, prolonged heat stress significantly decreases cell viability in a time-dependent manner. In our project, we used in-plate control to determine the effect of temperature on the cells.[78] Cell viabilities were calculated with respect to the appropriate in-plate control. We observed that the percent viability of B16F10 cells was reduced significantly from 89% to 77.5% at the minimum concentration tested during this experiment. Various pathological conditions, specifically inflammation and malignancies, are associated with the activation of immune cells to release various inflammatory markers that increase the local temperature at the site of inflammation and tumors.[79] The smart drug delivery systems that are able to release the drug in response to temperature variations act as targeted drug delivery systems and reduce off-site toxicities. The phase transition of nanocarriers at elevated temperatures (41°C and 43°C) to release the trapped drug may influence the uptake of the drug at the local site of the tumor other than body cells with normal body temperatures and hence improved cytotoxicities.[80] The tumor cells are more sensitive to temperature and permeability is significantly increased leading to improved delivery of nanoparticles. Dose-dependent toxicities can be avoided if the dose required to maintain the same cytotoxic effect is decreased. Li et al investigated mild hyperthermal dose effects (41°C for 1 hour in murine melanoma tumor models) on extravasation, penetration, and accumulation of liposomes. They found that this temperature did not damage tumor vasculature and produced a temporary alteration in the endothelial network.[81] Based on these findings, we aimed to provide a trigger for drug release from lipid nanocarriers following this protocol. The results demonstrated significant alteration in the amount of drug release and dose-dependent cytotoxicity after activating the lipid construct. Doxorubicin's intracellular uptake by passive diffusion may increase due to increased fluidity and permeability of the cell membrane. Mild hyperthermia favors the quick release of doxorubicin and enhanced cytotoxicity at specific tumor sites. However, the release of the drug at normothermia (37°C) was prolonged, and less cytotoxic potential was observed than the free drug. Similar findings demonstrating the effect of temperature on intracellular internalization and cytotoxicity were reported by Lokerse et al.[82]

Hemolytic Potential

The aggregation and deformation of red blood cells (RBCs) results in various circulatory disorders. Thus, the compatibility of nanoplatforms with blood is a crucial parameter for the successful development of nanocarriers. The size and concentration of nanoparticles may affect the degree of aggregation and hemolysis in red blood cells as reported by Kim and Shin.[83] The number of nanoparticles/mL of colloidal dispersions may also negatively affect the hemolysis potential.[31] A hemolytic potential of less than 10% is generally considered to be safe for the biomaterials intended for injection.[72] The maximum hemolytic activity observed in drug-loaded lipid nanocarriers was about 7% at the highest lipid concentration while blank nanocarriers exhibited less than 5% hemolysis at all studied concentrations. The

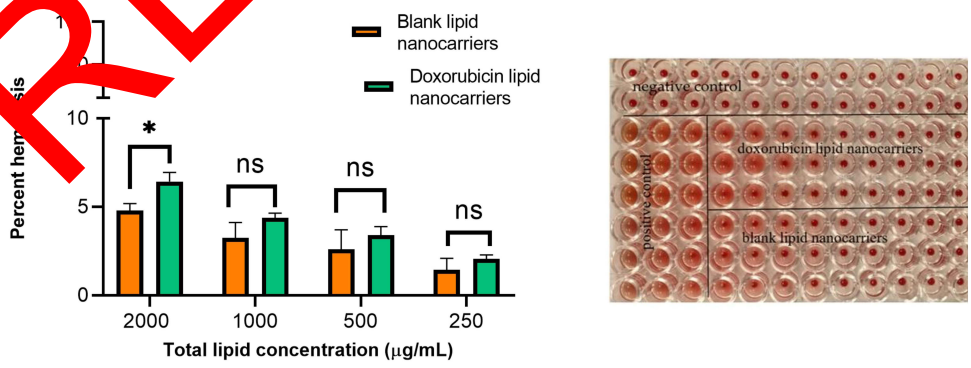

Figure 9 Right panel: qualitative presentation of in-vitro hemolysis potential of blank and doxorubicin-loaded lipid nanocarriers with saline as a negative control and 2% triton-x 100 in saline as a positive control. Left panel: hemolysis percentage of blank and doxorubicin lipid nanocarriers at 250–2000 µg/mL of total lipid concentration. Data are presented as mean± SD, n=3, *p < 0.05.
Abbreviation: ns, non-significant.

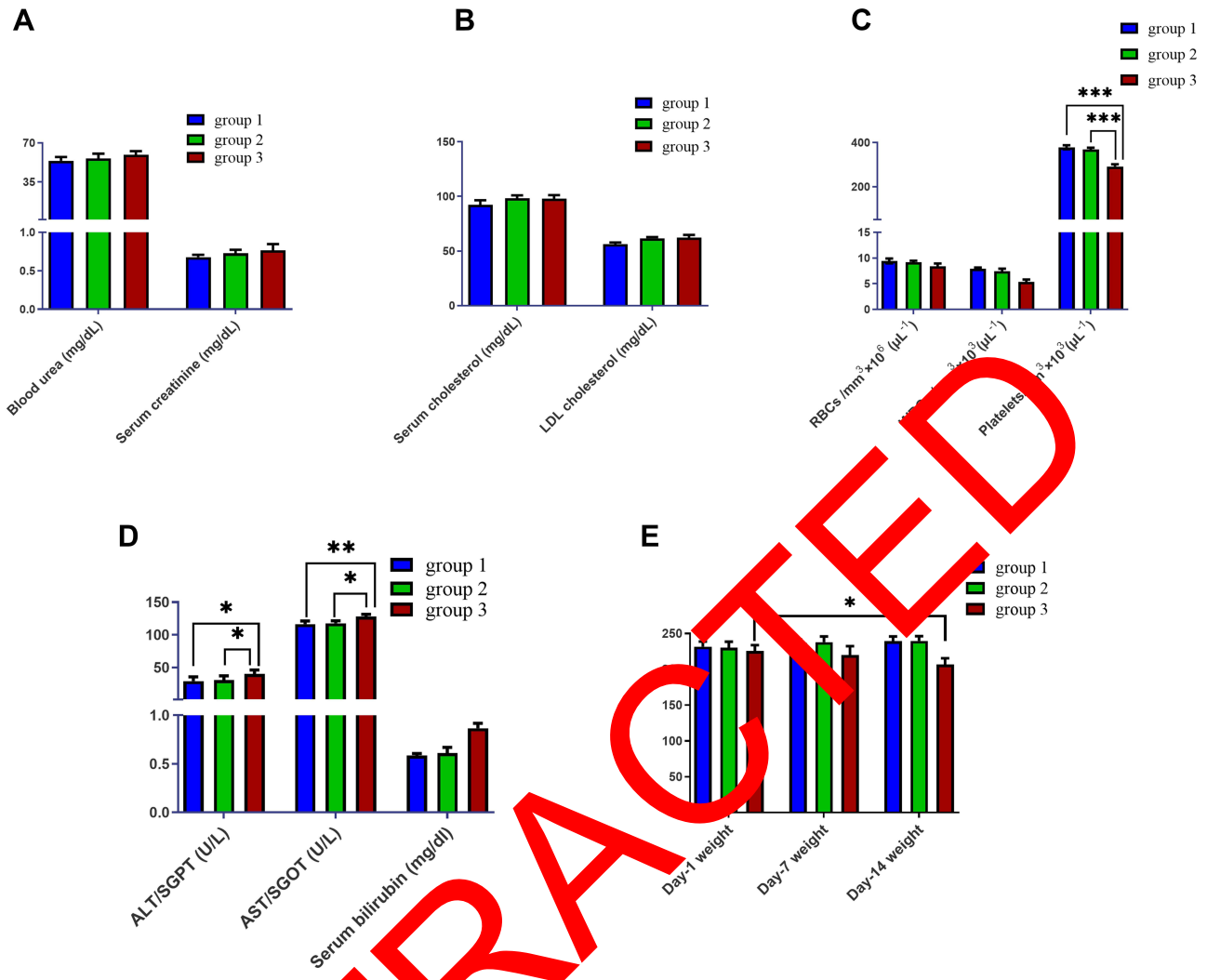

Figure 10 Analysis of biochemical and hem[illegible]ological parame[illegible]s in group-I as the control group, group-2 tested with blank lipid nanocarriers, and group-3 tested with doxorubicin-loaded lipid nanocarriers. (**A**[illegible] function test, (**B**[illegible]id profile, (**C**) hematological parameters, (**D**) liver function test, (**E**) total body weight changes. Data are presented as mean ± SD, n=3, *p < 0.[illegible], **p ≤ [illegible], ***p ≤ 0.001.

Abbreviations: LDL, low-density l[illegible]oprotein; RBC[illegible]d blood cells; WBC$_S$, white blood cells; ALT, alanine aminotransferase; SGPT, serum glutamic pyruvic transaminase; AST, aspartate aminotransferase[illegible]GOT, serum glutami[illegible]xaloacetic transaminase.

qualitative an[illegible]quanti[illegible]ve resul[illegible] suggested that our carriers had excellent hemocompatibility with erythrocytes when injected i[illegible]raven[illegible]sly (F[illegible]9 right and left panel).

Acute [illegible]icity Study

Different path[illegible]ogical markers including liver function, kidney function, hematology, lipid profile, and body weights were checked to determine the biosafety of the developed lipid nanocarriers and compared with control groups. The drug-free lipid nanocarriers have negligible effects when compared with control as all the results were statistically insignificant during analysis by two-way ANOVA followed by post hoc Tukey's multiple comparison test ($p > 0.05$) (Figure 10A–E). There was a significant drop in platelet count for group III treated with lipid nanocarriers loaded with doxorubicin. It is well established that chemotherapeutics specifically doxorubicin therapy is associated with decreased white blood cell and platelet counts due to myelosuppression. The same findings were reported by several researchers.[84,85]

The elevated alanine aminotransferase (ALT) and aspartate aminotransferase (AST) levels in group-III representing hepatocellular damage were supported by the patch necrosis seen histologically (Figure 11). Aminotransferases are released in blood in response to increased cellular membrane permeability caused by liver injury as found in the

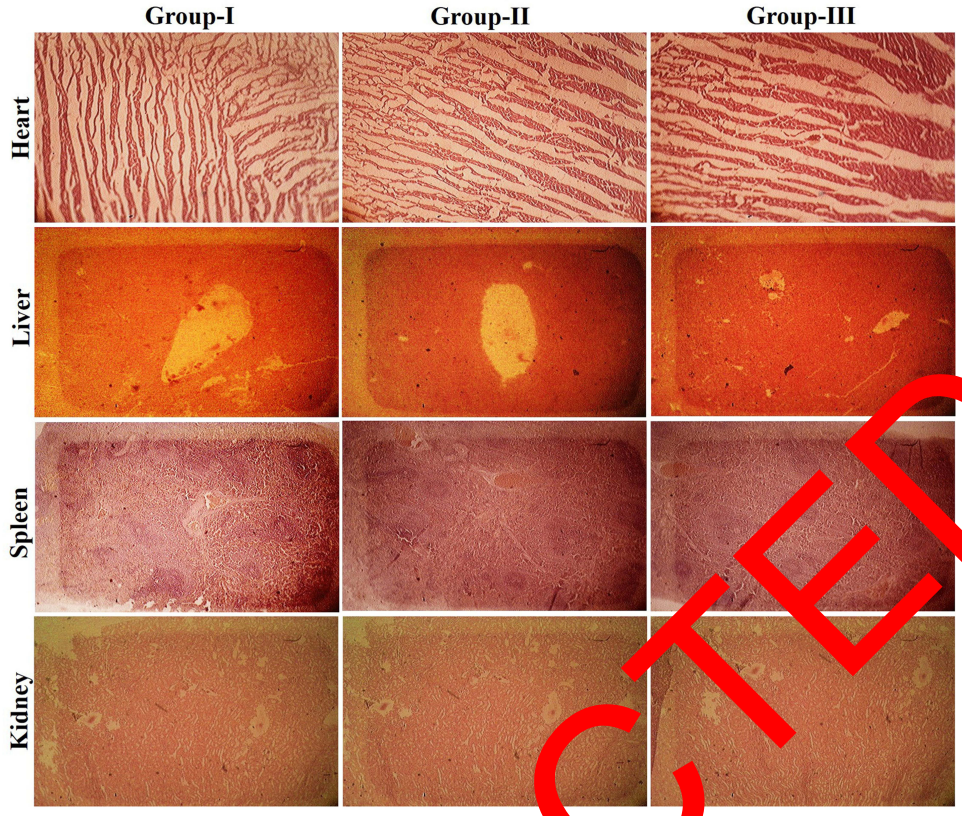

Figure 11 Histopathological analysis of heart, liver, spleen, and kidney of group-I animals as control treated with saline, group-II treated with carrier or blank lipid nanocarriers, group-III treated with doxorubicin-loaded lipid nanocarriers.

literature.[86] The liver-related toxicity induced by doxorubicin was presented in another study that reported co-delivery of doxorubicin, docosahexaenoic acid, and vitamin E by nanostructured lipid carriers and found a significant improvement in hepatic damage.[73] However, in our study, there were no macroscopic lesions in vital organs including the heart, kidney, liver, and spleen.

The histological slides of vital organs of group-II animals did not show any sign of toxicity when compared with control. No significant change in the weight of organs was observed at the time of sacrifice when compared with the control group. Body weight of group-III was significantly lower than control because the animals lost their appetite and got mild diarrhea-like symptoms due to chemotherapeutic effects as reported previously.[87] There was no significant change in body weight of group-II compared to the control group-I as these animals were taking a normal diet. No behavioral changes or deaths were recorded during this study. These findings support the safe and non-toxic nature of the developed formulation.

Conclusion

The findings of this study suggested that eutectic mixtures of fatty acids can be efficiently utilized as a lipid construct for colloidal drug delivery carriers. The melting point of lipid mixtures can be tuned to melt and release the encapsulated drug at desired temperature range. The physicochemical characterizations of developed carriers were associated with the optimum size distribution required for enhanced permeability and retention effects. The drug release and cytotoxicity of the drug at mild hyperthermic temperature conditions favor a specific tumor environment. These carriers appeared to be safe for biological applications and thus can be efficiently utilized to encapsulate different chemotherapeutics for temperature-triggered drug release applications. In the future, doxorubicin-loaded lipid nanocarriers may serve as a multifunctional platform for combination chemo-thermotherapy of cancer. The provision of controlled and homogenous level of hyperthermia play a critical role that may influence the targeted systemic delivery of therapeutic compounds from a temperature

responsive carrier. Magnetic resonance, high intensity focused ultrasound and radiofrequency ablation are common techniques to induce cancer cell death apoptosis in thermotherapy[88,89] without altering the tumor perfusion for chemotherapeutics. Doxorubicin-loaded lipid nanocarriers can be combined with thermotherapy wherein thermotherapy will not only induce cancer cell apoptosis but also release doxorubicin to kill the remaining cancer cells. Lipid nanocarriers proposed in this study can also load inorganic nanomaterials[23] that are used as contrast agents for magnetic resonance, near-infrared radiation and high intensity focused ultrasound.[90] Furthermore, cytotoxicity and thermoresponsive targeting of lipid nanocarriers must be performed in in-vivo cancer models to identify additional barriers, if any, and their potential for translation for human use. However, further studies are required to mimic the ex-vivo and in-vivo behavior of these carriers. These carriers can be explored in the future for active targeting and site-specific delivery for multiple chemotherapeutics.

Institutional Review Board Statement

The in vivo study was conducted according to the OECD (Organization for Economic Co-operation and Development) guidelines and approved by the "Pharmacy animals and ethics committee (PAEC; PAEC number is 22/2021-PAEC) of the Islamia University of Bahawalpur".

Acknowledgments

The authors acknowledge the Higher Education Commission of Pakistan for providing fellowship to author FP under Indigenous Ph.D. Scholarship (Pin # 417-58133-2MD4-025) and International Research Support Initiative Program (IRSIP 44 PSc 38) during this study at Northeastern University (Boston, M.A), USA. The authors would like to extend their sincere appreciation to Dr. William C. Hartner for their helpful comments during the preparation and language editing of the manuscript. The authors would like to thank Prof. Dr. Naveed Akhtar Pro-Vice-Chancellor and Dean Faculty of Pharmacy, The Islamia University of Bahawalpur for providing research facilities during this study.

Author Contributions

All authors have significantly contributed to the conception, study design, execution, and acquisition of data, analysis, and interpretation of the work reported. All authors took part in drafting, revising, or critically reviewing the article; gave final approval of the version to be published; have agreed on the journal to which the article has been submitted; and agree to be accountable for all aspects of the work.

Funding

This research received no external funding or grant except for two fellowships by the Higher Education Commission of Pakistan.

Disclosure

The authors report no conflicts of interest in this work.

References

1. World Health Organization. Key facts of cancer; 2018. Available from: https://www.who.int/news-room/fact-sheets/detail/cancer. Accessed December 18, 2019.
2. Sung H, Ferlay J, Siegel RL, et al. Global cancer statistics 2020: GLOBOCAN estimates of incidence and mortality worldwide for 36 cancers in 185 countries. *CA Cancer J Clin*. 2021;71(3):209–249. doi:10.3322/caac.21660
3. World Health Organization. Cancer; 2021. Available from: https://www.who.int/news-room/fact-sheets/detail/cancer. Accessed June 30, 2021.
4. Bray F, Ferlay J, Soerjomataram I, Siegel RL, Torre LA, Jemal A. Global cancer statistics 2018: GLOBOCAN estimates of incidence and mortality worldwide for 36 cancers in 185 countries. *CA Cancer J Clin*. 2018;68(6):394–424. doi:10.3322/caac.21492
5. Baudino TA. Targeted cancer therapy: the next generation of cancer treatment. *Curr Drug Discov Technol*. 2015;12(1):3–20. doi:10.2174/1570163812666150602144310
6. Subhan MA, Yalamarty SSK, Filipczak N, Parveen F, Torchilin VPJ. Recent advances in tumor targeting via EPR effect for cancer treatment. *J Pers Med*. 2021;11(6):571. doi:10.3390/jpm11060571
7. Liu D, Yang F, Xiong F, Gu N. The smart drug delivery system and its clinical potential. *Theranostics*. 2016;6(9):1306. doi:10.7150/thno.14858

8. Lyon PC, Gray MD, Mannaris C, et al. Safety and feasibility of ultrasound-triggered targeted drug delivery of doxorubicin from thermosensitive liposomes in liver tumours (TARDOX): a single-centre, open-label, phase 1 trial. *Lancet Oncol*. 2018;19(8):1027–1039. doi:10.1016/S1470-2045(18)30332-2
9. Dou Y, Hynynen K, Allen CJ. To heat or not to heat: challenges with clinical translation of thermosensitive liposomes. *J Control Release*. 2017;249:63–73. doi:10.1016/j.jconrel.2017.01.025
10. Pereira Gomes I, Aparecida Duarte J, Chaves Maia AL, et al. Thermosensitive nanosystems associated with hyperthermia for cancer treatment. *Pharmaceuticals*. 2019;12(4):171. doi:10.3390/ph12040171
11. Madni A, Sarfraz M, Rehman M, et al. Liposomal drug delivery: a versatile platform for challenging clinical applications. *J Pharm Pharm Sci*. 2014;17(3):401–426. doi:10.18433/J3CP55
12. Rehman M, Madni A, Shi D, et al. Enhanced blood brain barrier permeability and glioblastoma cell targeting via thermoresponsive lipid nanoparticles. *Nanoscale*. 2017;9(40):15434–15440. doi:10.1039/C7NR05216B
13. Shao P, Wang B, Wang Y, Li J, Zhang Y. The application of thermosensitive nanocarriers in controlled drug delivery. *J Nanomater*. 2011;2011:17. doi:10.1155/2011/389640
14. Vihola H, Laukkanen A, Valtola L, Tenhu H, Hirvonen J. Cytotoxicity of thermosensitive polymers poly (N-isopropylacrylamide), poly (N-vinylcaprolactam) and amphiphilically modified poly (N-vinylcaprolactam). *Biomaterials*. 2005;26(16):3055–3064. doi:10.1016/j.biomaterials.2004.09.008
15. Dunne M, Epp-Ducharme B, Sofias AM, Regenold M, Dubins DN, Allen C. Heat-activated drug delivery increases tumor accumulation of synergistic chemotherapies. *J Control Release*. 2019;308:197–208. doi:10.1016/j.jconrel.2019.06.012
16. World Health Organization. *WHA70.12: Cancer Prevention and Control in the Context of an Integrated Approach*. Geneva: World Health Assembly; 2017.
17. Rehman M, Asadullah Madni AI, Khan WS, et al. Solid and liquid lipid-based binary solid lipid nanoparticles of diacerein: in vitro evaluation of sustained release, simultaneous loading of gold nanoparticles, and potential thermoresponsive behavior. *Int J Nanomedicine*. 2015;10:2805. doi:10.2147/IJN.S67147
18. Wu J-Y, Liu S-Q, Heng PW-S, Yang -Y-Y. Evaluating proteins release from, and their interactions with, thermosensitive poly (N-isopropylacrylamide) hydrogels. *J Control Release*. 2005;102(2):361–372. doi:10.1016/j.jconrel.2004.10.008
19. Sosnik A, Cohn DJB. Reverse thermo-responsive poly (ethylene oxide) and poly (propylene oxide) multiblock copolymers. *Biomaterials*. 2005;26(4):349–357. doi:10.1016/j.biomaterials.2004.02.041
20. Bhattarai N, Ramay HR, Gunn J, Matsen FA, Zhang MJJo CR. PEG-grafted chitosan as an injectable thermosensitive hydrogel for sustained protein release. *JCREEC*. 2005;103(3):609–624. doi:10.1016/j.jconrel.2004.12.019
21. Brezaniova I, Hruby M, Kralova J, et al. Temoporfin-loaded 1-tetradecanol-based thermoresponsive solid lipid nanoparticles for photodynamic therapy. *J Control Release*. 2016;241:34–44. doi:10.1016/j.jconrel.2016.09.00
22. Chen Q, Zhu C, Huo D, et al. Continuous processing of phase-change materials for uniform nanoparticles for near-infrared-triggered drug release. *Nanoscale*. 2018;10(47):22312–22318. doi:10.1039/C8NR07027J
23. Rehman M, Madni A, Ihsan A, et al. Solid and liquid lipid-based binary solid lipid nanoparticles of diacerein: in vitro evaluation of sustained release, simultaneous loading of gold nanoparticles, and potential thermoresponsive behavior. *Int J Nanomedicine*. 2015;10:2805.
24. Vimala K, Sundarraj S, Paulpandi M, Vengatesan S, Kan SJ. Green synthesized doxorubicin loaded zinc oxide nanoparticles regulates the Bax and Bcl-2 expression in breast and colon carcinoma. *Process Biochem*. 2014;49(1):160–172.
25. Agbo CP, Ugwuanyi TC, Ugwuoke WI, McConville C, Attama AA, Ofokansi KC. Intranasal artesunate-loaded nanostructured lipid carriers: a convenient alternative to parenteral formulations for the treatment of severe and cerebral malaria. *J Control Release*. 2021;334:224–236. doi:10.1016/j.jconrel.2021.04.020
26. Alam S, Aslam M, Khan A, et al. Nanostructured lipid carriers of pioglitazone for transdermal application: from experimental design to bioactivity detail. *Drug Deliv*. 2016;23(2):601–6 10.3109/1071 44.2014.923958
27. ICH Harmonised Tripartite Guideline. Validation of analytical procedures: text and methodology. *Q2 (R1)*. 2005;1(20):05.
28. Pezeshki A, Hamishehkar H, anbarzadeh B, al. Nanostructured lipid carriers as a favorable delivery system for β-carotene. *Food Biosci*. 2019;27:11–17.
29. Keshri L, Pathak KJ. Development thermodynamically stable nanostructured lipid carrier system using central composite design for zero order permeation of econazole trate through epidermis. *Pharm Dev Technol*. 2013;18(3):634–644. doi:10.3109/10837450.2012.659256
30. Du Y, Ling L, Ismail M, et dox sensitive lipid-camptothecin conjugate encapsulated solid lipid nanoparticles for oral delivery. *Int J Pharma*. 2018;549(1–2): doi: 016/j. arm.2018.08.010
31. Mendes LP, elgado F, Costa , et al. Biodegradable nanoparticles designed for drug delivery: the number of nanoparticles impacts on cytotoxici *Toxicol in vitro*. 2015;29(6):1268–1274. doi:10.1016/j.tiv.2014.12.021
32. OECD. *Guideline 3: Acute Oral Toxicity-Acute Toxic Class Method*. OECD; 2001.
33. Pereverzeva E, eschalin I, Treschalin M, et al. Toxicological study of doxorubicin-loaded PLGA nanoparticles for the treatment of glioblastoma. *Int J Pharm*. 201 54:161–178. doi:10.1016/j.ijpharm.2018.11.014
34. de Oliveira Silva J, anda SEM, Leite EA, et al. Toxicological study of a new doxorubicin-loaded pH-sensitive liposome: a preclinical approach. *Toxicol Appl Pharmacol*. 2018;352:162–169. doi:10.1016/j.taap.2018.05.037
35. Zhang N, Yuan Y, Wang X, Cao X, Yang X, Hu S. Preparation and characterization of lauric–myristic–palmitic acid ternary eutectic mixtures/expanded graphite composite phase change material for thermal energy storage. *Chem Eng J*. 2013;231:214–219.
36. Zhang N, Yuan Y, Du Y, Cao X, Yuan Y. Preparation and properties of palmitic-stearic acid eutectic mixture/expanded graphite composite as phase change material for energy storage. *Energy*. 2014;78:950–956.
37. Sarı A. Eutectic mixtures of some fatty acids for low temperature solar heating applications: thermal properties and thermal reliability. *Arterioscler Thromb Vasc Biol*. 2005;25(14–15):2100–2107. doi:10.1161/01.ATV.0000183745.37161.6e
38. Zhu C, Huo D, Chen Q, Xue J, Shen S, Xia Y. A eutectic mixture of natural fatty acids can serve as the gating material for near-infrared-triggered drug release. *Adv Mater*. 2017;29(40):1703702.
39. Xue K, Lv S, Zhu C. Bringing naturally-occurring saturated fatty acids into biomedical research. *J Mater Chem B*. 2021;9(35):6973–6987. doi:10.1039/D1TB00843A

40. Doktorovová S, Araújo J, Garcia ML, Rakovský E, Souto E. Formulating fluticasone propionate in novel PEG-containing nanostructured lipid carriers (PEG-NLC). *Coll Surf B*. 2010;75(2):538–542. doi:10.1016/j.colsurfb.2009.09.033
41. Jan N, Madni A, Rahim MA, et al. In vitro anti-leukemic assessment and sustained release behaviour of cytarabine loaded biodegradable polymer based nanoparticles. *Life Sci*. 2021;267:118971. doi:10.1016/j.lfs.2020.118971
42. Rajaei A, Hadian M, Mohsenifar A, Rahmani-Cherati T, Tabatabaei M, Life S. A coating based on clove essential oils encapsulated by chitosan-myristic acid nanogel efficiently enhanced the shelf-life of beef cutlets. *Food Pack Shelf Life*. 2017;14:137–145.
43. Yi H, Zhan W, Zhao Y, et al. A novel core-shell structural montmorillonite nanosheets/stearic acid composite PCM for great promotion of thermal energy storage properties. *Env Monit Asses*. 2019;192:57–64. doi:10.1007/s10661-019-7899-9
44. Rai N, Madni A, Faisal A, et al. Glyceryl monostearate based solid lipid nanoparticles for controlled delivery of docetaxel. *Curr Drug Deliv*. 2021;18(9):1368–1376. doi:10.2174/1567201818666210203180153
45. Pezeshki A, Ghanbarzadeh B, Mohammadi M, Fathollahi I, Hamishehkar H. Encapsulation of vitamin A palmitate in nanostructured lipid carrier (NLC)-effect of surfactant concentration on the formulation properties. *Adv Pharm Bull*. 2014;4(Suppl 2):563. doi:10.5681/apb.2014.083
46. Chauhan I, Yasir M, Verma M, Singh AP. Nanostructured lipid carriers: a groundbreaking approach for transdermal drug delivery. *Adv Pharm Bull*. 2020;10(2):150. doi:10.34172/apb.2020.021
47. Roti Roti JL. Cellular responses to hyperthermia (40–46 C): cell killing and molecular events. *Int J Hyperthermia*. 2008;24(1):3–15. doi:10.1080/02656730701769841
48. Fernandes RS, Silva JO, Monteiro LO, et al. Doxorubicin-loaded nanocarriers: a comparative study of liposo[illegible]and nanostruc[illegible]ed lipid carrier as alternatives for cancer therapy. *Biomed Pharmacother*. 2016;84:252–257. doi:10.1016/j.biopha.2016.09.032
49. Taymouri S, Alem M, Varshosaz J, et al. Biotin decorated sunitinib loaded nanostructured lipid carrier[illegible]or tum[illegible]argeted che[illegible]otherapy of lung cancer. *J Drug Deliv Sci Technol*. 2019;50:237–247.
50. Gordillo-Galeano A, Mora-Huertas CE. Biopharmaceutics solid lipid nanoparticles and nanost[illegible]tured lipi[illegible]carriers:[illegible]view emphasizing on particle structure and drug release. *Eur J Pharma Biopharma*. 2018;133:285–308. doi:10.1016/j.[illegible]b.201[illegible]0.017
51. Patel VR, Agrawal YJ. Nanosuspension: an approach to enhance solubility of drugs. *J Ad[illegible]harm[illegible]ol Res*. 20[illegible];2(2):81.
52. Bhattacharjee SJ. DLS and zeta potential–what they are and what they are not? *Control R[illegible]ase*. 2[illegible]6;235:337–351. doi:10.1016/j.jconrel.2016.06.017
53. Bhadra A, Karmakar G, Nahak P, et al. Impact of detergents on the physiochemica[illegible]behavi[illegible]f itraconazole loaded nanostructured lipid carriers. *Coll Surf*. 2017;516:63–71.
54. Montoto SS, Sbaraglini ML, Talevi A, et al. Carbamazepine-loaded solid[illegible]id [illegible]noparticles and[illegible]nostructured lipid carriers: physicochemical characterization and in vitro/in vivo evaluation. *Coll Surf B*. 2018;167:7[illegible]81.
55. Bashiri S, Ghanbarzadeh B, Ayaseh A, Dehghannya J, Ehsani A, Ozyur[illegible]d. Essential oi[illegible]aded nanostructured lipid carriers: the effects of liquid lipid type on the physicochemical properties in beverage models. *Food [illegible]sci*. 2020;35:[illegible]0526.
56. Fernandes RS, Silva JO, Mussi SV, et al. Nanostructured lipid carrier co-lo[illegible]d with dox[illegible]ubicin and docosahexaenoic acid as a theranostic agent: evaluation of biodistribution and antitumor activity in experim[illegible]model. *Mol[illegible]Biol*. 2018;20(3):437–447. doi:10.1007/s11307-017-1133-3
57. Özdemir S, Çelik B, Üner M. Properties and therapeutic p[illegible]ential[illegible]olid lipid nanoparticles and nanostructured lipid carriers as promising colloidal drug delivery systems. In: *Materials for Biomedical [illegible]gineering*. [illegible]ier; 2019:457–505.
58. Oliveira MS, Goulart GCA, Ferreira LAM, Carn[illegible]GJE. H[illegible]nobic ion pairing as a strategy to improve drug encapsulation into lipid nanocarriers for the cancer treatment. *Expert O[illegible]Drug[illegible]Deliv*. 2[illegible]7;14(8):983–995. doi:10.1080/17425247.2017.1266329
59. Araujo VHS, da Silva PB, Szlachetka IO, et[illegible]The infl[illegible]nce of N[illegible]composition on curcumin loading under a physicochemical perspective and in vitro evaluation. *Coll Surf A*. 2020;602:[illegible]070.
60. Wassel RA, Grady B, Kopke RD, Dorr[illegible]KJ,[illegible]ochemical SA, Aspects E. Dispersion of super paramagnetic iron oxide nanoparticles in poly (d, l-lactide-co-glycolide) micropar[illegible]es. *Coll Su[illegible]*. 2007;292(2–3):125–130.
61. Kumar MR, Bakowsky U, Lehr[illegible]. Preparation a[illegible]characterization of cationic PLGA nanospheres as DNA carriers. *Biomaterials*. 2004;25(10):1771–1777.
62. Kayal S, Ramanujan RJ. Doxorubicin l[illegible]ed PVA coated iron oxide nanoparticles for targeted drug delivery. *Mater Sci Eng C*. 2010;30(3):484–490.
63. Yoncheva K, Tzank[illegible]B, Yorda[illegible]v Y, et al. Encapsulation of doxorubicin in chitosan-alginate nanoparticles improves its stability and cytotoxicity in resistant lymph[illegible]a L5178[illegible]MDR cells. *J Drug Deliv Sci Technol*. 2020;59:101870.
64. Patro NM, Devi K, [illegible]R, Suresh S[illegible]Evaluation of bioavailability, efficacy, and safety profile of doxorubicin-loaded solid lipid nanoparticles. *J Nanopar[illegible]*. 2013;15[illegible]2):1–18.
65. Yang K[illegible]Peng F[illegible]Wen Y[illegible]. Re-examination of characteristic FTIR spectrum of secondary layer in bilayer oleic acid-coated Fe3O4 nano[illegible]rticles. *Ap[illegible]Surf Sci*. 2[illegible]10;256(10):3093–3097.
66. Karim[illegible], Gh[illegible], Hamishehkar H, Mehramuz B, Kafil HS. Antioxidant, antimicrobial and physicochemical properties of turmeric extract-lo[illegible]a nanostructured lipid carrier (NLC). *Coll Interface Sci Commun*. 2018;22:18–24.
67. Islan GA, T[illegible]ello PC, Abraham GA, Duran N, Castro GR. Smart lipid nanoparticles containing levofloxacin and DNase for lung delivery. *Des Charact*. 2016;[illegible]:168–176.
68. Abdolahpour S, Mahdieh N, Jamali Z, Akbarzadeh A, Toliyat T, Paknejad M. Development of doxorubicin-loaded nanostructured lipid carriers: preparation, characterization, and in vitro evaluation on MCF-7 cell line. *BioNanoScience*. 2017;7(1):32–39.
69. Pinto F, de Barros DP, Reis C, Fonseca LP. Optimization of nanostructured lipid carriers loaded with retinoids by central composite design. *J Mol Liquids*. 2019;293:111468.
70. Borges GSM, de Oliveira Silva J, Fernandes RS, et al. Sclareol is a potent enhancer of doxorubicin: evaluation of the free combination and co-loaded nanostructured lipid carriers against breast cancer. *Life Sci*. 2019;232:116678. doi:10.1016/j.lfs.2019.116678
71. Xu X, Shan GR, Pan PJ. Controlled co-delivery of hydrophilic and hydrophobic drugs from thermosensitive and crystallizable copolymer nanoparticles. *J Appl Polymer Sci*. 2016;133(42). doi:10.1002/app.44132
72. Liu P, Wu Q, Li Y, et al. DOX-conjugated keratin nanoparticles for pH-sensitive drug delivery. *Coll Surf B*. 2019;181:1012–1018. doi:10.1016/j.colsurfb.2019.06.057

73. Lages EB, Fernandes RS, de Oliveira Silva J, et al. Co-delivery of doxorubicin, docosahexaenoic acid, and α-tocopherol succinate by nanostructured lipid carriers has a synergistic effect to enhance antitumor activity and reduce toxicity. *Biomed Pharmacother*. 2020;132:110876. doi:10.1016/j.biopha.2020.110876
74. Ferjaoui Z, Jamal Al Dine E, Kulmukhamedova A, et al. Doxorubicin-loaded thermoresponsive superparamagnetic nanocarriers for controlled drug delivery and magnetic hyperthermia applications. *ACS Appl Mater Interfaces*. 2019;11(34):30610–30620. doi:10.1021/acsami.9b10444
75. Lu T, Ten Hagen TL. A novel kinetic model to describe the ultra-fast triggered release of thermosensitive liposomal drug delivery systems. *J Control Release*. 2020;324:669–678. doi:10.1016/j.jconrel.2020.05.047
76. Ce R, Lavayen V, Couto GK, et al. Folic acid-doxorubicin-double-functionalized-lipid-core nanocapsules: synthesis, chemical structure elucidation, and cytotoxicity evaluation on ovarian (OVCAR-3) and bladder (T24) cancer cell lines. *Pharma Res*. 2021;38(2):301–317. doi:10.1007/s11095-021-02989-y
77. Zhao X, Chen Q, Liu W, et al. Codelivery of doxorubicin and curcumin with lipid nanoparticles results in improved efficacy of chemotherapy in liver cancer. *Int J Nanomed*. 2015;10:257. doi:10.2147/IJN.S73322
78. Gao S, Zhou A, Cao B, et al. A tunable temperature-responsive and tough platform for controlled drug delivery. *N J Chem*. 2021;45(29):13056–13063.
79. Carlin KJ. Autoimmune disease pH and temperature. *J Clin Med Res*. 2014;6(4):305.
80. Bolla PK, Rodriguez VA, Kalhapure RS, et al. A review on pH and temperature responsive gels and other less explored drug delivery systems. *J Drug Deliv Sci Technol*. 2018;46:416–435.
81. Li L, ten Hagen TL, Bolkestein M, et al. Improved intratumoral nanoparticle extravasation and penetration by mild hyperthermia. *J Control Release*. 2013;167(2):130–137. doi:10.1016/j.jconrel.2013.01.026
82. Lokerse WJ, Bolkestein M, Ten Hagen TL, et al. Investigation of particle accumulation, chemosensitivity and thermosensitivity for effective solid tumor therapy using thermosensitive liposomes and hyperthermia. *Theranostics*. 2016;6(10):1717.
83. Kim MJ, Shin SJF. Toxic effects of silver nanoparticles and nanowires on erythrocyte rheology. *Food Chem Toxicol*. 2014;67:80–86. doi:10.1016/j.fct.2014.02.006
84. Kitamura Y, Hattori S, Yoneda S, et al. Doxorubicin and cyclophosphamide treatment produces anxiety-like behavior and spatial cognition impairment in rats: possible involvement of hippocampal neurogenesis via brain-derived neurotrophic factor and dopamine D1 regulation. *Behav Brain Res*. 2015;292:184–193. doi:10.1016/j.bbr.2015.06.007
85. Desai VG, Herman EH, Moland CL, et al. Development of doxorubicin-induced chronic cardiotoxicity in the B6C3F1 mouse model. *Toxicol Appl Pharmacol*. 2013;266(1):109–121. doi:10.1016/j.taap.2012.10.025
86. Saleem U, Amin S, Ahmad B, Azeem H, Anwar F, Mary S. Acute oral toxicity evaluation of aqueous ethanolic extract of Saccharum munja Roxb. roots in albino mice as per. *OECD*. 2017;4:580–585.
87. Goodwin SC, Bittner CA, Peterson CL, Wong G. Single-dose toxicity study of hepatic intra-arterial infusion of doxorubicin coupled to a novel magnetically targeted drug carrier. *Toxicolog Sci*. 2001;60(1):177–183. doi:10.1093/toxsci/60.1.177
88. Swenson CE, Haemmerich D, Maul DH, Knox B, Ehrhart N, Subramanian RA. Increased duration of heating boosts local drug deposition during radiofrequency ablation in combination with thermally sensitive liposomes (ThermoDox) in a porcine model. *PLoS One*. 2015;10(10):e0139752. doi:10.1371/journal.pone.0139752
89. Lyon PC, Mannaris C, Gray M, et al. Large-volume hyperthermia for safe and cost-effective targeted drug delivery using a clinical ultrasound-guided focused ultrasound device. *Ultrasound Med Biol*. 2021;47(4):982–997. doi:10.1016/j.ultrasmedbio.2020.12.008
90. Wu D, Jin X, Wang X, et al. Engineering temperature-sensitive platelet liposomes as a tailored chemotherapy platform in combination with HIFU ablation for cancer treatment. *Theranostics*. 2019;9(13):3962–3979. doi:10.7150/thno.32172